Sustainable Transesterification of Cellulose with High Oleic Sunflower Oil in a DBU-CO 2 Switchable Solvent

Kelechukwu Onwukamike, Stéphane Grelier, Etienne Grau, Henri Cramail, Michael Meier

Sustainable Transesterification of Cellulose with High Oleic Sunflower Oil in a DBU-CO_2 Switchable Solvent

Kelechukwu N. Onwukamike, Stéphane Grelier, Etienne Grau, Henri Cramail*, Michael A. R. Meier*

Abstract :

The direct transesterification of cellulose with high oleic sunflower oil, without any activating steps, was achieved in a DBU-CO_2 solvent system to obtain fatty acid cellulose esters (FACEs). Optimization of the reaction parameters (i.e., concentration, temperature, plant oil equivalents, as well as reaction time) was performed using microcrystalline cellulose (MCC) and followed by Fourier-transform infrared spectroscopy (FT-IR). Further confirmation of the FACEs structures was achieved via ^{1}H and ^{13}C NMR, and ^{31}P NMR revealed DS (degree of substitution) values of up to 1.59. The optimized conditions were successfully applied to filter paper (FP) and cellulose pulp (CP). Characterization of the FACEs showed improved thermal stability after transesterification reactions (up to 30 °C by TGA) and a single broad 2θ peak around 19.8° by XRD, which is characteristic of a more amorphous material. In addition, films were prepared via solvent casting and their mechanical properties obtained from tensile strength measurements, revealing an elastic modulus (*E*) of up to 478 MPa with elongation of about 35% and a maximum stress of 22 MPa. The film morphology was studied by scanning electron microscopy (SEM) and showed homogeneous surfaces. In this report, we thus demonstrated a more sustainable approach toward FACEs that combines cellulose and plant oil (two renewable resources) directly, resulting in fully renewable polymeric materials with appealing properties.

Synopsis

The direct transesterification of cellulose with plant oils in a CO_2 switchable solvent system leads to polymeric materials with desirable properties in a sustainable fashion.

Introduction

Sustainability entails the utilization of available resources without jeopardizing their use for future generations. Fossil-based resources do not fulfill this requirement, and their additional negative environmental impacts explain the increasing valorization efforts of renewable raw materials. Naturally occurring biopolymers, such as cellulose, starch, or chitin/chitosan offer interesting application possibilities and are therefore considered as sustainable alternatives to fossil resources, especially for polymer chemistry. These biopolymers are a major part of the over 170×10^9 tons of lignocellulosic biomass that are produced annually.(1,2) As cellulose constitutes between 35 and 50% of this amount,(1,3,4) it is therefore the most abundant biobased organic polymer.(5) Furthermore, only about 3% of cellulose is utilized in nonfood applications such as pulp and paper industries,(6) thus leaving a sizable percentage as a sustainable raw material for new applications. Cellulose is a linear homopolymer of β-1,4 linked D-glucopyranose units.(5) In addition to its abundance, cellulose exhibits very good thermal and mechanical stability and high hydrophilicity and is biodegradable and biocompatible.(5) However, due to its inherent strong intra- and intermolecular hydrogen bonding, it is insoluble in common organic solvents as well as in water,(5) and the absence of any thermal transition makes it nonprocessable. Thus, in order to introduce solubility and processability to cellulose, the chemical modification of the three OH groups (per anhydroglucose unit (AGU)) of cellulose represents an interesting strategy.(7,8)

Two routes can be explored for the chemical modification of cellulose, i.e., heterogeneous and homogeneous derivatization. Heterogeneous modification of cellulose is widely employed industrially for the synthesis of cellulose derivatives, as it is easier to perform and solubility of cellulose is not a requirement. It has been

employed for the synthesis of commercially available cellulose derivatives such as cellulose esters (cellulose triacetate),(9) cellulose ethers (carboxymethylcellulose, CMC),(8) and cellulose silyl ethers (trimethylsilylcellulose, TMSC).(10) Using such processes, the degree of substitution (DS) of the cellulose structure is not easily controlled. In cellulose acetate for example, a DS of 3 is usually achieved, and deacetylation is necessary to obtain lower DS values. Furthermore, the stoichiometric use of reagents, the use of strong bases/acids to swell/activate the cellulose backbone, as well as the generation of waste during the synthesis affect the sustainability of the process. In order to have a better control of the modified cellulose structure, the homogeneous modification is preferred, even if it involves the challenging solubilization of cellulose as a first step. Generally, solubility of cellulose can be achieved in solvents capable of breaking its inherent intra- and intermolecular hydrogen bonds.(5) Two main classes of cellulose solvents are so-called nonderivative and derivative solvents.

In nonderivative solvents, the functionalization of cellulose occurs after the solubilization step. Examples include *N*,*N*-dimethylacetamide-lithium chloride (DMAc-LiCl),(11)*N*-methylmorpholine *N*-oxide (NMMO),(12) and dimethyl sulfoxide-tetramethylammonium fluoride (DMSO-TBAF).(13) These solvents suffer from limitations such as difficult recovery and/or toxicity. However, successful homogeneous modifications including esterification,(14−16) etherification,(17) and cellulose grafting (from or onto)(18) have been reported in these solvents. Another class of nonderivative solvents are ionic liquids, such as 1-butyl-3-methylimidazolium chloride (BMIMCl).(19) The latter are considered as “greener” alternatives due to their very low vapor pressure and the possibility to recycle and reuse the solvent after the reaction. Since the first report from Swatloski et al., many approaches have been reported on the homogeneous modification of cellulose in ionic liquids.(20) However, their use is limited by their high cost and the noninertness of some ionic liquids, such as 1-ethyl-3-methylimidazolium acetate (EMIMAc), making their recovery more challenging.(21)

On the other hand, in derivative solvents, the solubilization of cellulose proceeds through a prefunctionalization that enables solubilization. A well-known example is the viscose process. In this case, the native cellulose is first transformed into alkali cellulose, which can react with CS_2 to highly viscous xanthogenates (i.e., viscose), which can be processed into films or fibers.(5) Whereas this process remains the most employed route for making cellulose fibers, the use of toxic CS_2 as well as the inherent challenge of treating the wastewater is unsustainable. A more sustainable derivative solvent system has been recently reported and involves the derivatization of cellulose to a DMSO soluble carbonate anion using CO_2 in the presence of a super base.(22,23) Compared to the viscose process, it is less toxic and easier to recycle since the process is reversible. Esterification(24) and grafting from cellulose using lactides(25) are examples of recent homogeneous modifications of cellulose in this solvent system. Furthermore, we recently showed the efficiency of this solvent system for the succinylation of cellulose, achieving a DS of 2.59 under very mild reaction conditions (room temperature, 30 min).(26)

Cellulose esters are among the most investigated and produced cellulose derivatives finding applications in the coating industry and as optical media films.(5) Typically, these substrates are produced industrially via heterogeneous modification. However, several investigations via homogeneous routes have been reported using activated acid derivatives (i.e., acid chlorides or anhydrides) in stoichiometric amounts. In the context of green chemistry, the use of renewable resources is not enough, but rather the entire synthesis process should be considered to ensure sustainability.(27) In a more sustainable approach, acid anhydrides and acyl chlorides should be substituted by esters that are easier to handle, less toxic, and noncorrosive and result in less waste upon esterification. In this regard, we reported the catalytic transesterification of cellulose using methyl esters and fatty acid methyl ester (FAMEs) resulting to formation of FACEs (fatty acid cellulose esters) in the ionic liquid BMIMCl with TBD as catalyst.(28) Even though moderate degrees of substitution (DS) of 0.69 were reached, it did pave the way for a more sustainable approach for synthesizing cellulose esters. Films made from FACEs have been investigated as sustainable packaging materials.(29,30) In both reports, fatty acid chlorides were used and the cellulose modification was carried under heterogeneous conditions. Kilpelainen et al. showed that such FACE films had good water vapor and air barrier properties with improved mechanical properties.(29) However, the

use of acid chlorides as well as the use of pyridine for swelling the cellulose in this report makes the process less sustainable. Hence, producing FACEs by direct utilization of plant oils would improve the sustainability of this transesterification process by avoiding derivatization steps. In this regard, we succeeded to carry out catalytic transesterification of starch using plant oils (high oleic sunflower oil and olive oil) in DMSO with TBD as catalyst reaching a DS of 1.3.(31) The obtained fatty acid starch esters were soluble in most organic solvents and showed good mechanical properties. However, utilizing starch raises the debate about "food or fuel" due to its very important role as food. Thus, replacing starch with cellulose will address this concern. Furthermore, the highly linear structure and higher molecular weight of cellulose is a challenge in terms of processing on the one hand but should result in materials with improved mechanical properties.

So far, the only report on utilizing plant oils directly for cellulose modification is from Dankovich and Hseih.(32) The authors heterogeneously modified cellulose (cotton) surfaces using several plant oils (soybean, rapeseed, olive, coconut, and sunflower oil) in order to increase the hydrophobicity of the fibers. The procedure involved first solubilizing the plant oils in acetone or ethanol and then allowing cellulose (cotton) to swell in this solution, after which the solvents were removed and samples heated between 110 and 120 °C for 1 h to improve the surface modification. However, there is no report on homogeneous modification of cellulose using plant oils directly, the advantages of which were highlighted above. Herein, we thus focus on the direct transesterification of cellulose with plant oils in the DMSO–CO_2-DBU switchable solvent system. Apart from DBU, also TBD would be a suitable catalyst for this type of reaction, which can also directly react with CO_2.(31,34) However, DBU is cheaper and, most importantly, a liquid and thus easier handle and to recover in this switchable solvent process. To show the scope of our developed protocol, we investigated three cellulose sources: microcrystalline cellulose (MCC), cellulose filter paper (FP), and cellulose pulp (CP) using high oleic sunflower oil without any pretreatment. The reaction conditions were optimized and a thorough characterization of the obtained materials revealed improved properties compared to similar materials reported previously and prepared via less sustainable approaches.

Experimental Section

Materials

Microcrystalline cellulose (MCC, Sigma-Aldrich) and cellulose (Whatman filter paper, No. 5) were used. Cellulose pulp was purchased from Rayonier Advanced Materials Company (Tartas Biorefinery, France) and was produced by ammonium sulphite cooking and bleached with an elementary chlorine free (ECF) process (purity in alpha-cellulose is 94%). All cellulose samples were dried at 100 °C for 24 h under vacuum to remove free water before use. The following chemicals were used without further purification: 2-chloro-4,4,5,5-tetramethyl-1,3,2-dioxaphospholane (2-Cl-TMDP, 95%), deuterated chloroform ($CDCl_3$-*d*), deuterated dimethyl sulfoxide (DMSO-d_6), deuterated tetrahydrofuran (THF-d_8) and were purchased from Merck. *endo*-*N*-Hydroxy-5-norbornene-2,3-dicarboximide (97%, Sigma-Aldrich) and diazabicyclo[5.4.0]undec-7-ene (DBU, >98%) were purchased from TCI. In addition, carbon dioxide was purchased from Air Liquid (CO_2 > 99.9%) and dimethyl sulfoxide (DMSO) from VWR (99%). High oleic sunflower oil was purchased from T + T Oleochemie GmbH, 63755 Alzenau, Germany. In addition, isopropanol and tetrahydrofuran (THF) were of technical grade and used without further purification.

General Procedure for the Synthesis of Fatty Acid Cellulose Esters (FACEs)

Cellulose (0.25 g, 1.5 mmol, 5 wt %) was stirred in DMSO (5 mL) followed by addition of DBU (0.7 g, 4.6 mmol, 3 eq. per anhydroglucose unit). The cloudy suspension was transferred to a steel pressure reactor, where 5 bar of CO_2 was applied at 30 °C for 15 min, after which the obtained clear cellulose solution was transferred to a round-bottom flask. High oleic sunflower oil (3 equiv triglycerides per AGU, 4.0 g, 5 mmol) was added and stirred vigorously, and the reaction was performed at 115 °C from 6 to 24 h depending on the experiment. Afterward, the obtained hot homogeneous mixture was added dropwise into 200 mL of isopropanol. The obtained precipitate was filtered and washed twice with isopropanol (2 × 100 mL). After filtration, the precipitate was solubilized in THF (10 mL) and reprecipitated in distilled water (250 mL) to remove any remaining DBU and DMSO.

The final precipitate obtained after filtration was dried under vacuum at 60 °C for 24 h leading to a white fibrous material as the final product. The same procedure was employed for the other cellulose sources (filter paper and cellulose pulp). Yields obtained ranged from 65 to 80%.

ATR-IR: ν (cm^{-1}) = 3466–3395 ν(O–H), 3004 ν(═C–H), 2921–2884 ν_s(C–H), 1740 ν(C═O) of esters, 1160 ν(C–O), 1025–1050 ν(C–O) glycopyranose of cellulose. ^{1}H NMR (400 MHz, DMSO-d_6, 90 °C, 1024 scans) δ (ppm) = 5.34 (br, 2H), 5.24–3.01 (m, AGU, 7H), 2.75 (m, 2H), 2.31 (m, 2H), 2.0 (m, 4H), 1.55 (m, 2H), 1.28 (m, 28H), 0.87 (m, 3H). ^{13}C NMR (100 MHz, DMSO-d_6, 90 °C, 6000 scans) δ (ppm) = 172.18, 129.22, 127.60, 102.41, 79.81, 74.50, 72.87, 60.22, 32.82, 30.80, 30.46, 28.69, 28.58, 28.37, 28.16, 26.22, 24.86, 23.99, 21.55, 13.33.

Instruments

IR Spectroscopy

Infrared spectra of all samples were recorded on a Bruker alpha-p instrument using ATR technology within the range from 4000 to 400 cm^{-1} with 24 scans.

Nuclear Magnetic Resonance Spectroscopy (NMR)

^{1}H NMR spectra were recorded using a Bruker Prodigy spectrometer operating at 400 MHz at 90 °C (DMSO-d_6) and at 50 °C (THF-d_8) with 1024 scans and a time delay d_1 of 1 s. Data were reported in ppm relative to DMSO-d_6 (2.5 ppm) and THF-d_8 (1.73 and 3.58 ppm). ^{13}C NMR spectra were recorded using a Bruker Prodigy spectrometer operating at 100 MHz at 90 °C (DMSO) and 50 °C (THF-d_8) with 6000 scans and a time delay d_1 of 2 s. Data are reported in ppm relative to DMSO-d_6 (39.52 ppm) and THF-d_8 (25.49 and 67.57 ppm). All products were dissolved with the concentrations of 10–20 mg/mL.

^{31}P NMR Method for DS Determination

Degree of substitutions (DS) were determined by ^{31}P NMR using a Bruker Ascend 400 MHz spectrometer with 1024 scans, a delay time d_1 of 5 s, and a spectral width of 90 ppm (190–100 ppm). Samples were prepared according to the following procedure: An exact amount of 25 mg of a sample was weighted and dissolved in 0.5–1 mL of pyridine. Next, 1–1.5 mL of $CDCl_3$ was added together with 2-chloro-4,4,5,5-tetramethyl-1,3,2-dioxaphospholane (2-Cl-TMDP, 100 µL, 0.63 mmol). The solution was allowed to homogenize, after which the internal standard, *endo*-*N*-hydroxy-5-norbornene-2,3-dicarboximide (150 µL, 123.21 mM in pyridine/$CDCl_3$ = 3:2, 0.0154 mmol) was added and the solution was stirred for further 30 min. Then, 600 µL of the solution was transferred to an NMR tube. DS values were calculated according to the reported equation.(33)

Size Exclusion Chromatography (SEC)

For samples with a DS of about 1.0, measurements were performed using a SEC system with DMAc (0.008 g L^{-1} LiBr) as eluent, whereas THF was used for samples with higher DS. A sample concentration of 2 g L^{-1} was used, and measurements were performed on a Polymer Laboratories PL-GPC 50 Plus Integrated System containing an autosampler, a PLgel 5 µm bead-size guard column (50 × 7.5 mm), followed by three PLgel 5 µm Mixed-C columns (300 × 7.5 mm), and a refractive index detector at 50 °C with a flow rate of 1 mL min^{-1}. The system was calibrated against poly(methyl methacrylate) standards with molecular weights ranging from 700 to 2 × 10^6 Da. The dissolved samples were filtered through polytetrafluorethylene (PTFE) membranes with a pore size of 0.2 µm prior to injection.

Thermogravimetric Analysis (TGA)

TGA measurements were performed using a TGA Q-500 from TA Instruments. The FACE samples (about 10 mg) were heated from 25 to 900 °C under N_2 at a heating rate of 10 °C/min. After the measurements, weight loss was

calculated in order to determine the degradation temperature ($T_{d,5\%}$ and $T_{d,95\%}$) of the samples. $T_{d,5\%}$ is the temperature, at which 5% weight loss of the sample occurred, while $T_{d,95\%}$ is defined as temperature at which over 95% of the weight loss of sample occurred.

X-ray Diffraction (XRD) Measurements

X-ray diffraction (XRD) patterns were collected on a PANalitycal X'pert MPD-PRO Bragg–Brentano θ–θ geometry diffractometer equipped with a secondary monochromator and an X'celerator detector over an angular range of 2θ = 8–80°. Each acquisition lasted for 1 h and 27 min. The Cu Kα radiation was generated at 45 kV and 40 mA (λ = 0.15418 nm). The regenerated cellulose samples were prepared on silicon wafer sample holders (PANalytical zero background sample holders) and flattened with a piece of glass.

Scanning Electron Microscopy (SEM)

The surface morphologies of the prepared FACEs films were measured using a Hitachi TM-1000 tabletop microscope. Prior to the measurements, the films were made conducting by metallization using Au (30 s, 35 mA).

Film Preparation

Fatty acid cellulose esters (FACEs) films were prepared by dissolving the products in THF (3–4 wt %) and casting the solution into Teflon plates (100 × 20 mm). The films were formed after the solvent evaporated at room temperature for at least 48 h to ensure complete removal of the solvent, followed by drying under vacuum at 30 °C for 5 h. The film thickness (0.04 to 0.06 mm) was measured using a digital Vernier caliper.

Tensile Strength Measurement

The films were prepared into bone shapes (25 × 4 mm), and the tensile strength was measured using a GABO EXPLEXOR instrument with a 25N sensor. The initial speed was set at 5 mm/min. Three to five measurements were performed for each sample, and the standard deviation was calculated.

Results and Discussion

Taking into account our previous works on the transesterification of starch with plant oils(31) and the modification of carbohydrate in the CO_2-DBU switchable ionic liquid solvents,(26,35) we investigated the homogeneous transesterification of cellulose using plant oils (high oleic sunflower oil) without any prior purification/modification in a CO_2-DBU switchable solvent system (Scheme 1).

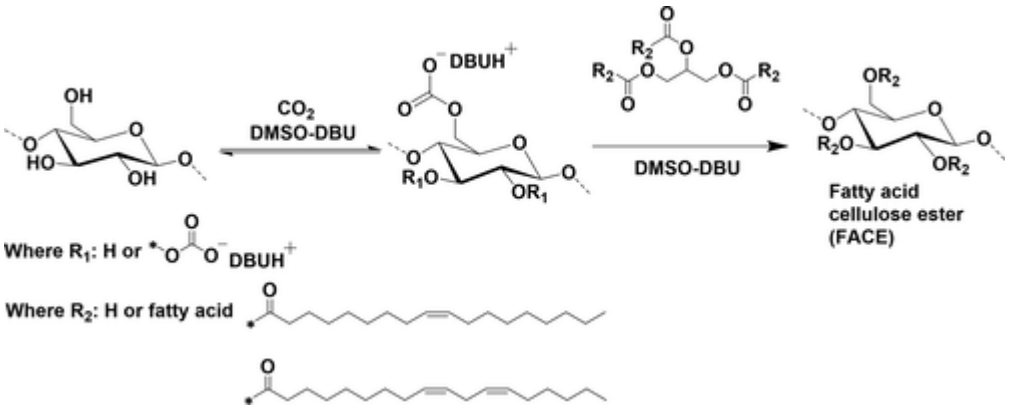

Scheme 1. Cellulose Solubilization in DBU-DMSO–CO_2 Switchable Solvent System and Subsequent Transesterification Using High Oleic Sunflower Oil

From our previous works on transesterification of carbohydrates (cellulose(28) and starch(31)) using an organic base (TBD) as the catalyst, 115 °C was observed as the optimal temperature. Thus, for the present study, this temperature was chosen. Prior to the transesterification reaction, cellulose was solubilized applying 5 bar of CO_2 in the presence of DBU (3 equiv per anhydroglucose unit of cellulose) and DMSO. The completion of the reaction was monitored via FT-IR (Figure 1). The FT-IR spectra were normalized to the C–O absorption of the pyranose unit in the cellulose backbone, which is not affected during cellulose modification (about 1025–1050 cm^{-1}) in order to compare the various investigated parameters relative to each other. After the transesterification, the appearance of the C═O absorbance band characteristic for the newly formed ester group at 1740 cm^{-1} was observed. In addition, the intensity of the O–H stretching bands on the cellulose backbone (about 3300 cm^{-1}) was significantly reduced and shifted toward higher wavenumbers (about 3400 cm^{-1}), indicating a decrease in hydrogen bonding in the cellulose backbone. Furthermore, the C–H stretching absorbance bands of CH_2 and CH_3 (2850 to 2925 cm^{-1}) corresponding to the aliphatic chain of the plant oils were observed. The peak at 1160 cm^{-1} is assigned to the C–O stretching band of the newly formed ester bond. In addition, the peak at about 3004 cm^{-1} is attributed to the ═C–H stretching band found in oleic acid, which is a major constituent of high oleic sunflower oil (Figure 1).

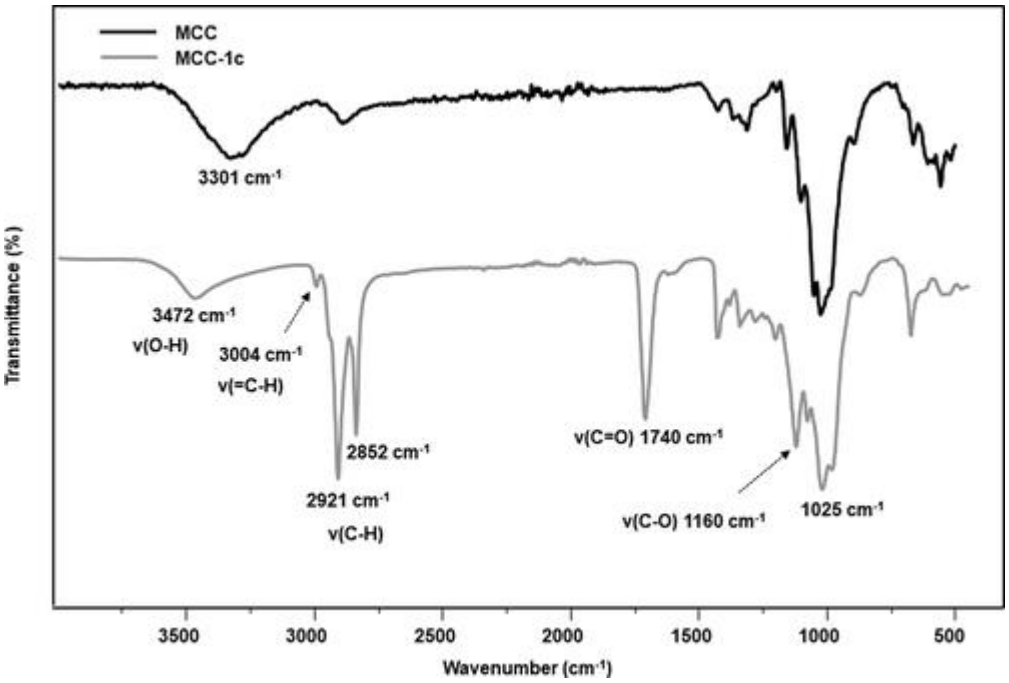

Figure 1. Typical FT-IR spectrum of a fatty acid cellulose ester, MCC-1c (5 wt % MCC, 3 equiv high oleic sunflower oil/AGU, 115 °C, 24 h) in comparison to native MCC.

Typically, transesterification reactions proceed through an equilibrium reaction, thus requiring the removal of one of the products to drive the reaction. The use of catalysts can help to reach this equilibrium faster. Previously, we reported on the catalytic transesterification of cellulose using methyl esters with the reaction driven both by the removal of methanol and the presence of TBD as a catalyst.(28) For the CO_2-DBU solvent system, we observed that only about 70% DBU is utilized during the solubilization step of cellulose,(35) thus being available to catalyze the transesterification reaction. In addition, more DBU catalyst is freed during the reaction as CO_2 is removed in the course of the reaction. We observed that the addition of the plant oil to the solubilized cellulose mixture first led to a biphasic mixture, which gradually became homogeneous as the reaction proceeded, as the formed mono- and diglycerides can act as amphiphiles, thus addressing the initial miscibility issue. The presence of such mono- and diglycerides upon transesterification were also observed in our previous work on transesterification of starch using plant oils.(31)

The optimization of reaction parameters was studied using microcrystalline cellulose (MCC). First, the effect of cellulose concentration was investigated, which was varied from 3 to 5 wt %, and the reaction was performed at 115 °C for 24 h using high oleic sunflower oil (3 equiv per AGU). After normalizing the spectra as mentioned above, the intensity of the C═O absorbance band from the fatty acid cellulose esters (FACEs; 1740 cm^{-1}) were compared to each other as presented in Figure 2, revealing that higher cellulose concentrations led to higher degrees of modification as evidenced by the increasing C═O absorbance intensities (Figure 2, right side). This is a typical observation, as most organic reactions proceed more efficiently in concentrated solutions.

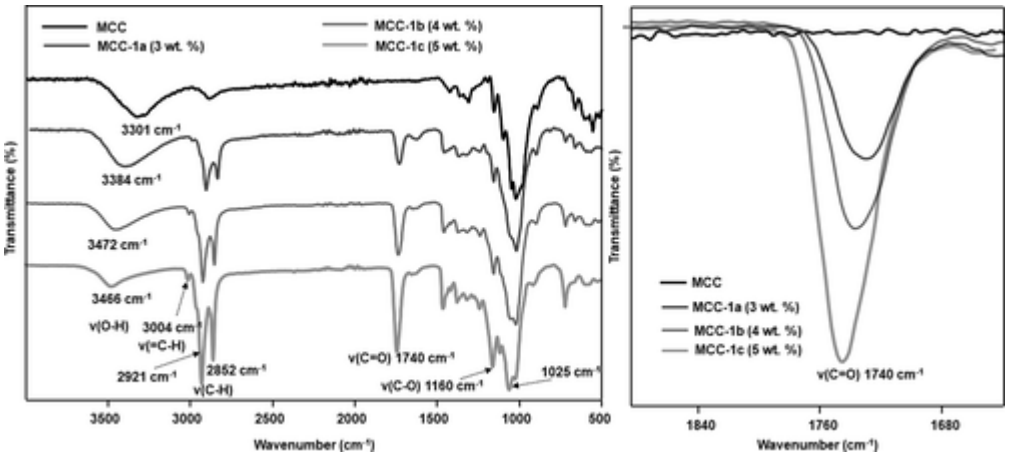

Figure 2. FT-IR spectra of FACEs obtained using high oleic sunflower oil at various cellulose (MCC) concentrations: 3 wt % (MCC-1a), 4 wt % (MCC-1b), and 5 wt % (MCC-1c). Peaks were normalized to the C–O absorbance of the pyranose units at 1025 cm^{-1} (3 equiv high oleic sunflower oil/AGU, 115 °C, 24 h).

In addition, an associated decrease in the O–H absorbance band (3300 cm^{-1}) was observed. Higher cellulose concentrations were not investigated, since the associated viscosity was too high for our experimental setup but might be worthwhile investigating in the future.

Another important parameter to investigate is the reaction time. Using 5 wt % MCC at 115 °C and 3 equiv of high oleic sunflower oil/AGU, the reaction time was varied between 6 and 48 h (Supporting Information, Figure S1). Results show that, up to 24 h (MCC-1c), conversion increased with a slight decrease observed at longer reaction times, indicating degradation and/or hydrolysis of the cellulose backbone and the formed esters, respectively. Furthermore, three different reaction temperatures (90, 100, and 115 °C) were investigated. Using 5 wt % cellulose (MCC), the reactions were performed for 24 h. The FT-IR results are presented in the Supporting Information (Figure S2). The results show that increasing the temperature led to a considerable increase in the conversion, which is due to an increased miscibility and an accelerated reaction. In terms of sustainability, the plant oil equivalents per anhydroglucose unit employed in the reaction is an important parameter. Thus, we investigated this parameter by varying the plant oil equivalents from 1.5 to 6 equiv triglycerides per AGU of cellulose in the transesterification reaction carried out at 115 °C and 24 h (Figure S3). We observed that increasing the plant oil equivalents from 1.5 to 3 led to a pronounced increase in the intensity of the C═O absorbance band (1740 cm^{-1}). In addition, as seen in Figure S3, there was no apparent difference in conversion when 6 equiv of plant oil (triglycerides) were employed. Thus, from a sustainability point of view, using such high excess of the plant oil was not justifiable.

Further confirmation of the structure of the FACEs was obtained from ^{1}H and ^{13}C NMR. As a typical example, the NMR results for the experiment performed for 6 h are presented (Figure 3). The vinylic protons of the oleic acid are observed at a chemical shift of 5.34 ppm in ^{1}H NMR, which is slightly moved toward the lower field compared to high oleic sunflower oil (5.19 ppm). The peaks between 5.26 and 3.07 ppm are attributed to the protons of the cellulose backbone. In the ^{13}C NMR spectrum, the carbonyl carbon of the ester in the plant oil (162.50 ppm) is moved further downfield to 172.24 ppm in the FACEs due to the change in its environment. The carbon of the unsaturated aliphatic chain from oleic acid (129.22 ppm) is also visible. The attributed peaks are similar to previous reports on heterogeneously modified cellulose using fatty acids (oleic acid).(29)

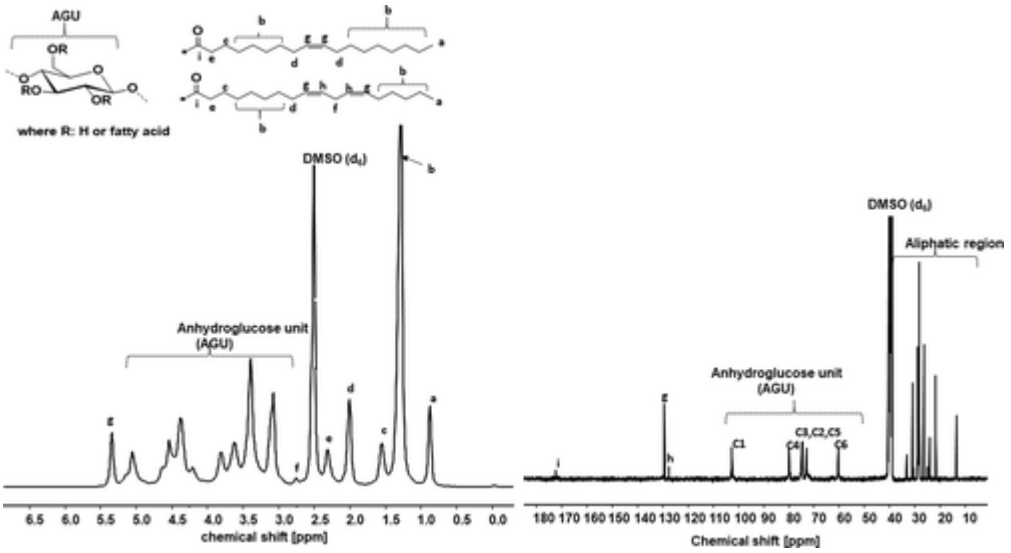

Figure 3. ^{1}H (left, 1024 scans, 400 MHz) and ^{13}C (right, 6000 scans, 100 MHz) NMR (DMSO-d_6) at 90 °C for FACE, MCC-1d, 5 wt % cellulose, 3 equiv high oleic sunflower oil/AGU, 115 °C, 6 h.

One pertinent advantage of homogeneous cellulose modification over its heterogeneous alternative is the ability to tune the degree of substitution (DS) by varying reaction parameters. The DS of the synthesized FACEs were determined via ^{31}P NMR (see the Experimental Section). The unreacted hydroxyl groups of the cellulose reacted with a phosphorylating agent as shown by the broad peak between 145 and 137 ppm in the ^{31}P NMR spectrum. The integration of this peak with respect to an internal standard allows the calculation of the DS according to a reported procedure.(33) The ^{31}P NMR data are displayed in the Supporting Information (Figures S4–8). The results obtained showed that the DS can be varied from 0.34 to 1.59 as the reaction time was increased from 6 to 24 h. The complete results are presented in the Supporting Information (Table S1). In addition, it was possible to tune the DS from 1.06 to 1.59 by varying the plant oil equivalence from 1.5 to 3 equiv per AGU of cellulose. The reactions carried out at 90 and 100 °C led to lower conversions. These samples could not be solubilized for DS calculation. This ability to tune the DS value over a wide range using various reaction parameters is interesting in order to target specific material properties. Overall, the highest value with a DS of 1.59 was reached after 24 h at 115 °C. Longer reaction times or higher temperatures (130 °C) did not increase the DS. This might be due to the increasing steric hindrance introduced by the long aliphatic groups, thus preventing further modification.

In order to investigate the effect of the cellulose source as well as the conversion (DS) on the material properties of the obtained FACEs, we synthesized two different DS samples (DS ∼1.0 and above 1.4) from each cellulose source: microcrystalline cellulose (MCC), cellulose pulp (CP), and cellulose Whatman filter paper No. 5 (FP). This was achieved by varying the plant oil equivalents (1.5 and 3 equiv triglycerides per AGU of cellulose) at 115 °C for 24 h. The FT-IR spectra of the obtained fatty acid cellulose esters (FACEs) are presented in the Supporting Information (see Figures S3, S9, and S10). The results obtained showed that the reaction efficiency does not depend on the type of cellulose used. The synthesized FACEs using 3 equiv of plant oils were soluble in THF, thus allowing further confirmation of the structures via ^{1}H and ^{13}C NMR (Figures S11a,b, S12a,b, S13a,b). The results are similar to those previously shown in Figure 3. However, we observed that the higher conversions in these samples led to much stronger aliphatic peaks from the plant oil. This made the cellulose backbone less visible, despite the high temperature (50 °C) and large number of scans (6000 scans for ^{13}C and 1024 scans for ^{1}H) employed during the NMR measurements. However, from the ^{13}C NMR, the characteristic vinylic protons (130.68 ppm) and carbonyl carbon atoms (173.36 ppm) of the introduced fatty acids are visible. Furthermore, we determined the degree of substitution (DS) of all the six synthesized FACEs (Table1), as previously described from ^{31}P NMR (see Figures S6, S8, S14, S15, S16, and S17). In addition, the relative weight-averaged molecular weights (M_W) of the synthesized fatty acid cellulose esters (FACEs) were determined from size exclusion chromatography (SEC) in dimethylacetamide-lithium bromide (DMAc-LiBr) for samples with DS of around 1.0 and

in THF for higher DS samples (see Table1). All measurements were performed relative to poly(methyl methacrylate) (PMMA) standards. The SEC traces of the measurements in THF are presented in Figure 4, and those in DMAc-LiBr (lower DS samples) are included in the Supporting Information (Figure S18). As seen from Figure 4, the highest molecular weights (M_W) were obtained for cellulose filter paper (190.0 kDa) followed by cellulose pulp (132.0 kDa) with microcrystalline cellulose having the lowest molecular weight (89.0 kDa). The dispersity (*Đ*) values ranged from 1.67 to 3.3. Higher values were obtained for measurements performed in DMAc-LiBr compared to those in THF. This difference is likely due to the difference in the swelling behavior of the polymers in these solvents. Furthermore, as expected from Table1, among the same cellulose source, higher molecular weights were obtained for samples with higher DS values (MCC-1c, FP-1b, and CP-1b). This can be attributed to the higher hydrodynamic radius with an increasing amount of long aliphatic side chains that are associated with increasing conversion (DS). However, it is important to point out that, since the measurements for the lower DS samples were performed in DMAc-LiBr instead of THF, it is difficult to directly compare these results with each other.

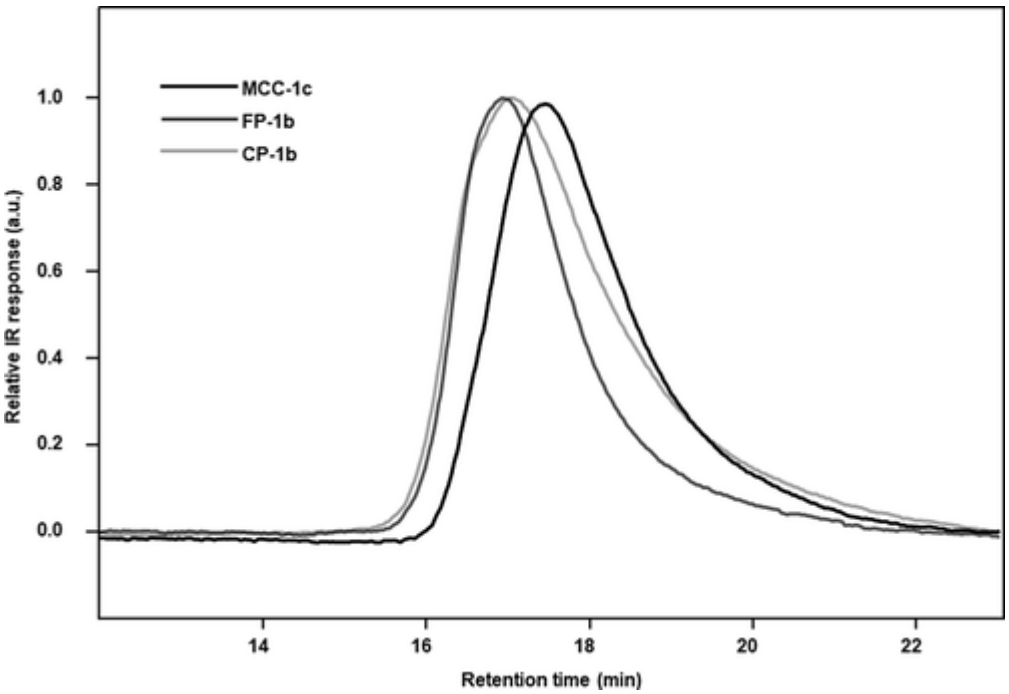

Figure 4. SEC traces (THF) of fatty acid cellulose esters (FACEs) from microcrystalline cellulose (MCC-1c; DS 1.59), cellulose Whatman filter paper No. 5 (FP-1b; DS 1.48), and cellulose pulp (CP-1b; DS 1.40).

Table 1. SEC Data, Degree of Substitution (DS) Values, Degradation Temperature (T_d), and XRD Data of FACEs

sample	DS[a]	M_n[b] (KDa)	M_w[b] (KDa)	Đ[b]	$T_{d,5\%}$[c] (°C)	$T_{d,95\%}$[c] (°C)	XRD[d] (2θ) (deg)
MCC					**280**	**340**	**22.6, 15.4**
MCC-1i	**1.06**	**63.4**	**167.3**	**2.6**	**302**	**363**	**19.6**
MCC-1c	**1.59**	**89.0**	**170.0**	**1.89**	**320**	**373**	**19.7**
FP					**298**	**350**	**22.8, 15.1**
FP-1a	**1.02**	**100.6**	**330.9**	**3.3**	**312**	**366**	**19.7**
FP-1b	**1.48**	**190.0**	**318.0**	**1.67**	**329**	**373**	**19.7**
CP					**261**	**355**	**22.6, 15,9**
CP-1a	**1.08**	**132.1**	**779.0**	**2.7**	**317**	**369**	**19.5**
CP-1b	**1.40**	**139.0**	**263.0**	**1.90**	**327**	**379**	**19.3**

[a]Determined from ^{31}P NMR.[b]Obtained from SEC measurements in THF or DMAc-LiBr.[c]Calculated from thermogravimetric analysis (TGA).[d]Obtained from X-ray diffraction measurements.

In addition, we investigated the crystal structure (crystallinity) of the various cellulose sources and their resulting FACEs by X-ray diffraction experiments. The results from microcrystalline cellulose (MCC) and the resulting FACEs (MCC-1c, MCC-1i) are shown in Figure 5. For comparison purposes, we have included the result of regenerated cellulose from a CO_2-DBU solvent system. We observed that, after transesterification, the characteristic cellulose I crystal 2θ peaks at 15.4° and 22.6° disappear and are replaced by a broad 2θ peak at around 19.8° that is characteristic for a less crystalline cellulose (more amorphous) as previously reported.(22) As seen from Figure 5 for the regenerated cellulose, the 2θ peaks (12.2°, 20.1°, and 21.6°), which are characteristic of the cellulose II crystalline phase, are clearly visible. We can explain these observed changes in the cellulose crystal structure by considering that during the solubilization of cellulose, the breaking of intra- and intermolecular hydrogen bonds result in a more amorphous structure. In the case of regeneration (in antisolvents like water), the cellulose chains are able to reorganize to the cellulose II crystal structure (thermodynamically more stable).(5) However, as observed from Figure 5, the transesterification process obviously prevented the reorganization of the cellulose chains after solubilization, thus mostly retaining the amorphous cellulose structure. Similar amorphous XRD diffraction patterns were obtained for cellulose Whatman filter paper No. 5

(FP-1a, FP-1b) and cellulose pulp (CP-1a, CP-1b; Figures S19, S20). The 2θ peaks of all of the FACEs investigated are included in Table1.

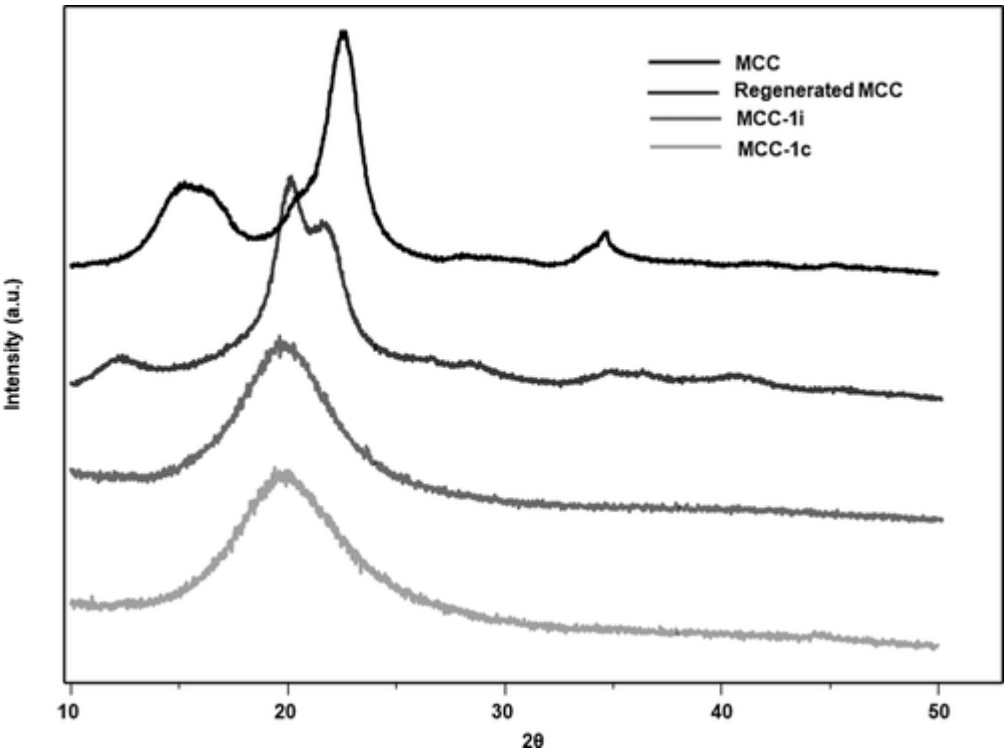

Figure 5. X-ray diffraction pattern of microcrystalline cellulose (MCC), regenerated MCC, and FACEs resulting from microcrystalline cellulose (MCC-1c, MCC-1i).

The thermal stability of the samples was determined by thermogravimetric analysis (TGA). The samples were heated from 25 to 900 °C (10 °C/min) under N_2 atmosphere. The result for $T_{d,5\%}$ and $T_{d,95\%}$ are shown in Table1. Typically, all of the samples showed a single major degradation step resulting in over 95% weight loss. Generally, the obtained results (see Table1 and Figures S21–23) showed an improved thermal stability after transesterification reactions (up to 30 °C), as higher DS samples resulted in a relatively higher thermal stability for all cellulose sources. For instance, for MCC the onset degradation temperature ($T_{d,5\%}$) was increased from 280 to 302 and 320 °C for DS 1.06 and 1.59, respectively. We observed similar trends in the case of cellulose Whatman filter paper No. 5 and cellulose pulp (see Table1). In the case of $T_{d,95\%}$, the degradation temperature of MCC was increased from 340 to 363 °C (DS 1.06) and 373 °C (DS 1.59). The $T_{d,95\%}$ of cellulose Whatman filter paper No. 5 (350 °C) increased to 366 °C (DS 1.02) and 373 °C (DS 1.48). Equally, the $T_{d,95\%}$ of cellulose pulp (355 °C) was increased to 369 °C (DS 1.08) and 379 °C (DS 1.40).

Since one of the aims of modifying cellulose using plant oils is to introduce processability to the material, we therefore prepared films from the six FACEs via a solvent cast method. The FACEs with a DS of about 1.0 were not soluble in THF, and thus films were prepared from pyridine solutions (MCC-F-1i, FP-F-1a, and CP-F-1a). It has to be noted that solvent casting can certainly not be considered sustainable, but it was the best possible option here to establish important material properties. In the future, of course, other processing option have to be considered. The films of FACEs with a higher DS were prepared in THF (MCC-F-1c, FP-F-1b, and CP-F-1b). As shown in Figure 6a, the obtained films showed good transparency.

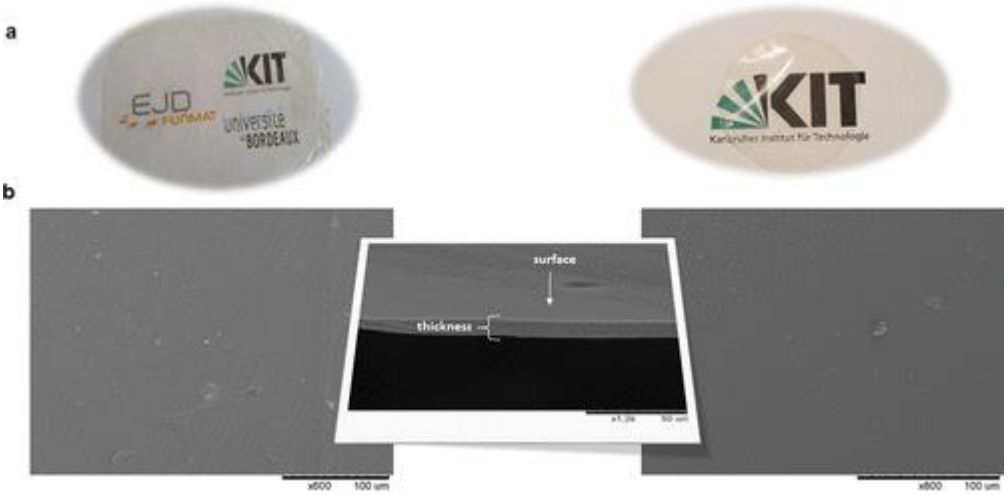

Figure 6. (a) Images of thin films of FACEs from MCC-F-1c (right) and CP-F-1b (left). (b) SEM surface images of MCC-F-1c (right), FP-F-1b (TS section with surface in view, middle), and CP-F-1b (left). (Films made via solvent cast from solubilized FACEs in THF).

The surface morphology of the films was determined via scanning electron microscopy (SEM). Results showed homogeneous surfaces without any holes (see Figure 6b). The transverse section (TS) is also visible (Figure 6b, middle), again confirming the homogeneous nature of the prepared films. The results obtained for all of the other FACEs films analyzed did not show any difference between samples from different cellulose sources or with different DS values.

Furthermore, the thermal stability of the films was determined using thermogravimetric analysis (TGA), the results are presented in the Supporting Information (Figure S24) and are included in Table2. Generally, the films show a single degradation step with similar degradation temperature ($T_{d,95\%}$) values comparable to their preceding precursors, thus showing that the materials did not lose their thermal stability during the film formation. It was also observable that, irrespective of the cellulose samples, thermal stability was influenced by the DS. Generally, films from higher DS samples exhibited a slightly higher thermal degradation temperature ($T_{d,5\%}$ and $T_{d,95\%}$). All FACE films analyzed had relatively high $T_{d,5\%}$ between 273 to 307 °C and $T_{d,95\%}$ between 359 to 368 °C, thus showing the improved thermal stability of the prepared films when compared to the starting cellulose samples (MCC $T_{d,5\%}$ = 280 °C, $T_{d,95\%}$ = 340 °C; FP $T_{d,5\%}$ = 298 °C, $T_{d,95\%}$ = 350 °C; CP $T_{d,5\%}$ = 261 °C, $T_{d,95\%}$ = 355 °C). This result is consistent with our previous observations on the increased stability introduced by the aliphatic side chain from the plant oil (see Figures S21–23 and compare to Figure S24).

Table 2. Thermal and Mechanical Characterization of Fatty Acid Cellulose Esters (FACEs) Cast Films

sample	$T_{d,5\%}$[a] (°C)	$T_{d,95\%}$[a] (°C)	Young's modulus,[b] E (MPa)	maximum stress[b] (MPa)	elongation at break,[b] strain (%)
MCC-F-1i	**298**	**367**	**375 ± 4**	**16 ± 2**	**27 ± 3**
MCC-F-1c	**307**	**368**	**233 ± 20.**	**16.19 ± 0.5**	**33.57 ± 1.8**
FP-F-1a	**291**	**360**	**458.38 ± 29.0**	**21.04 ± 1.4**	**30.54 ± 2.0**
FP-F-1b	**292**	**362**	**444.58 ± 23.6**	**21.96 ± 2.4**	**27.62 ± 1.7**
CP-F-1a	**273**	**359**	**478.26 ± 30.6**	**21.69 ± 2.3**	**27.70 ± 3.2**
CP-F-1b	**282**	**362**	**262.12 ± 13.53**	**15.89 ± 1.7**	**30.07 ± 0.9**

[a]Evaluated from thermogravimetric analysis (TGA).[b]Determined from tensile strength measurements.

Furthermore, we performed tensile strength measurements on the FACEs films. For each sample, three to five measurements were performed, and the average values of maximum stress (δ) and strain (%) including their standard deviations were calculated and are shown in Table2. The stress–strain curves of the various FACE films are displayed in Figure 7.

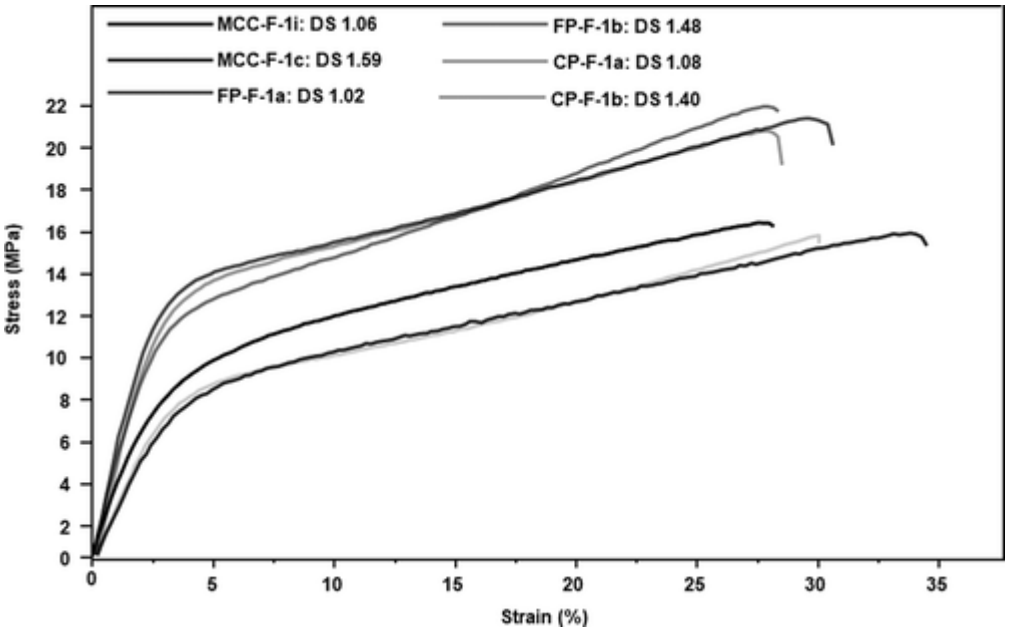

Figure 7. Tensile strength measurements of FACEs films (initial speed at 5 mm/min).

The elastic or Young's modulus (*E*) was determined from the linear region of the stress–strain curves. The average value from three to five measurements was calculated, and their standard deviation was determined (see Table2).

As seen in Figure 7 and Table2, a higher Young's modulus (*E*) was obtained for films with lower DS. In the MCC films for example, *E* decreased from 375 to 233 MPa as the DS increased from 1.06 to 1.59. This may be due to the higher remaining amount of free hydroxyl groups, which are able to hydrogen bond. The same reason could explain the slightly higher elongation values (over 30%) obtained for films with higher DS values, as the increasing presence of aliphatic side groups from the fatty acids increases the flexibility. Among the investigated cellulose samples, cellulose pulp showed the highest value of *E* (478 MPa) followed by cellulose filter paper (458 MPa) and microcrystalline cellulose (376 MPa). The latter lower value is most likely a result of the significantly lower molecular weight of the MCC samples. In addition, cellulose filter paper and cellulose pulp showed similar maximum stress values (around 22 MPa). The observed values of maximum stress are considerably higher compared to reported values for FACEs made via heterogeneous modification using fatty acid chloride from soybean oil (maximum stress between 1.7 to 2.4 MPa).(30) Furthermore, our obtained values of E are significantly higher than those reported for FACE films made via heterogeneous modification of cellulose using oleic acid chloride (*E* = 50.13 MPa).(29) We can therefore conclude that the direct combination of both plant oil and cellulose under homogeneous conditions led to FACE films with improved plasticity and mechanical strength. These improved mechanical properties are interesting for potential applications in packaging as well as other cellulose-based materials.

Conclusions

We have reported a sustainable approach for the homogeneous transesterification of cellulose using plant oils (high oleic sunflower oil) directly in the CO_2-DBU solvent system. The solubility of cellulose was accomplished within 15 min at 30 °C. Subsequent transesterification was performed at 115 °C for 24 h reaching a maximum degree of substitution (DS) of 1.59. No further catalyst was employed in the transesterification reaction, as the unreacted DBU from the solubilization step played a catalytic role. Compared to previous works where fatty acid methyl esters were used, the direct utilization of plant oils prevents derivatization steps, thus meeting one of the goals of green chemistry. Furthermore, we could show the possibility to tune the DS from 0.34 to 1.59 by

changing the reaction parameters. In addition, we showed the versatility of our developed protocol on various cellulose sources: microcrystalline cellulose (MCC), cellulose Whatman filter paper No. 5 (FP), and cellulose pulp (CP). The obtained FACEs showed improved thermal stability ($T_{d,95\%}$ up to 30 °C). From XRD measurements, a single broad 2θ peak at around 19.8° characteristic of the amorphous cellulose phase was obtained for all synthesized FACEs. Finally, films produced from these FACEs showed good thermal stability ($T_{d,95\%}$ over 360 °C) as well as high elastic moduli (up to 478 MPa), maximum stress of about 22 MPa, and maximum elongation (strain) of about 35%. The homogeneity of the films was confirmed with scanning electron microscopy (SEM). Hence, with this study, we have introduced a more sustainable approach for the modification of cellulose using plant oils directly. The developed protocol offers the possibility of tuning the DS over a wide range as well as the possibility for a further post modification via the double bonds on the introduced fatty acid backbone.

Acknowledgments

The authors thank Dr. Eric Lebraud for the XRD measurements and Daniel Zimmermann for assistance during the tensile strength measurements. K.N.O. would like to thank the EU for Ph.D. funding under the Horizon 2020 Marie Curie ITN Project EJD-FunMat (Project ID: 641640). H.C. and M.A.R.M. are also thankful for this funding.

References

1. Rose, M.; Palkovits, R. Cellulose-based sustainable polymers: State of the art and future trends. *Macromol. Rapid Commun.* **2011**, *32*, 1299– 1311, DOI: 10.1002/marc.201100230
2. Zhang, Y.-H. P. Reviving the carbohydrate economy via multi-product lignocellulose biorefineries. *J. Ind. Microbiol. Biotechnol.* **2008**, *35*, 367– 375, DOI: 10.1007/s10295-007-0293-6
3. Putro, J. N.; Soetaredjo, F. E.; Lin, S.-Y.; Ju, Y.-H.; Ismadji, S. Pretreatment and conversion of lignocellulose biomass into valuable chemicals. *RSC Adv.* **2016**, *6*, 46834– 46852, DOI: 10.1039/C6RA09851G
4. Delidovich, I.; Hausoul, P. J. C.; Deng, L.; Pfützenreuter, R.; Rose, M.; Palkovits, R. Alternative Monomers Based on Lignocellulose and Their Use for Polymer Production. *Chem. Rev.* **2016**, *116*, 1540– 1599, DOI: 10.1021/acs.chemrev.5b00354
5. Klemm, D.; Heublein, B.; Fink, H.-P.; Bohn, A. Cellulose: Fascinating biopolymer and sustainable raw material. *Angew. Chem., Int. Ed.* **2005**, *44*, 3358– 3393, DOI: 10.1002/anie.200460587
6. Kamm, B.; Kamm, M. Principles of biorefineries. *Appl. Microbiol. Biotechnol.* **2004**, *64*, 137– 145, DOI: 10.1007/s00253-003-1537-7
7. Kalia, S.; Kaith, B. S.; Kaur, I., Eds.; *Cellulose fibers: Bio- and nano-polymer composites: green chemistry and technology*; Springer: Berlin, **2011**.
8. Varshney, V. K.; Gupta, P. K.; Naithani, S.; Khullar, R.; Bhatt, A.; Soni, P. L. Carboxymethylation of α-cellulose isolated from Lantana camara with respect to degree of substitution and rheological behavior. *Carbohydr. Polym.* **2006**, *63*, 40– 45, DOI: 10.1016/j.carbpol.2005.07.001
9. Chen, C.-Y.; Chen, M.-J.; Zhang, X.-Q.; Liu, C.-F.; Sun, R.-C. Per-O-acetylation of cellulose in dimethyl sulfoxide with catalyzed transesterification. *J. Agric. Food Chem.* **2014**, *62*, 3446– 3452, DOI: 10.1021/jf5002233
10. Mormann, W. Silylation of Cellulose with Hexamethyldisilazane in Ammonia – Activation, Catalysis, Mechanism, Properties. *Cellulose* **2003**, *10*, 271– 281, DOI: 10.1023/A:1025100829371
11. McCormick, C. L.; Dawsey, T. R. Preparation of cellulose derivatives via ring-opening reactions with cyclic reagents in lithium chloride/N,N-dimethylacetamide. *Macromolecules* **1990**, *23*, 3606– 3610, DOI: 10.1021/ma00217a011
12. Fink, H.-P.; Weigel, P.; Purz, H. J.; Ganster, J. Structure formation of regenerated cellulose materials from NMMO-solutions. *Prog. Polym. Sci.* **2001**, *26*, 1473– 1524, DOI: 10.1016/S0079-6700(01)00025-9
13. Heinze, T.; Dicke, R.; Koschella, A.; Kull, A. H.; Klohr, E.-A.; Koch, W. Effective preparation of cellulose derivatives in a new simple cellulose solvent. *Macromol. Chem. Phys.* **2000**, *201*, 627– 631, DOI: 10.1002/(SICI)1521-3935(20000301)201:6<627::AID-MACP627>3.0.CO;2-Y
14. Tosh, B.; Saikia, C. N.; Dass, N. N. Homogeneous esterification of cellulose in the lithium chloride-N,N-dimethylacetamide solvent system: Effect of temperature and catalyst. *Carbohydr. Res.* **2000**, *327*, 345– 352, DOI: 10.1016/S0008-6215(00)00033-1
15. Morgado, D. L.; Rodrigues, B. V. M; Almeida, E. V. R.; Seoud, O. A. E.; Frollini, E. Bio-based Films from Linter Cellulose and Its Acetates: Formation and Properties. *Materials* **2013**, *6* (6), 2410– 2435, DOI: 10.3390/ma6062410

16. Ass, B. A. P.; Frollini, E.; Heinze, T. Studies on the homogeneous acetylation of cellulose in the novel solvent dimethyl sulfoxide/tetrabutylammonium fluoride trihydrate. *Macromol. Biosci.* **2004**, *4*, 1008– 1013, DOI: 10.1002/mabi.200400088
17. Hu, H.; You, J.; Gan, W.; Zhou, J.; Zhang, L. Synthesis of allyl cellulose in NaOH/urea aqueous solutions and its thiol–ene click reactions. *Polym. Chem.* **2015**, *6*, 3543– 3548, DOI: 10.1039/C5PY00301F
18. Roy, D.; Semsarilar, M.; Guthrie, J. T.; Perrier, S. Cellulose modification by polymer grafting: A review. *Chem. Soc. Rev.* **2009**, *38*, 2046– 2064, DOI: 10.1039/b808639g
19. Swatloski, R. P.; Spear, S. K.; Holbrey, J. D.; Rogers, R. D. Dissolution of Cellose with Ionic Liquids. *J. Am. Chem. Soc.* **2002**, *124*, 4974– 4975, DOI: 10.1021/ja025790m
20. Mäki-Arvela, P.; Anugwom, I.; Virtanen, P.; Sjöholm, R.; Mikkola, J. P. Dissolution of lignocellulosic materials and its constituents using ionic liquids—A review. *Ind. Crops Prod.* **2010**, *32*, 175– 201, DOI: 10.1016/j.indcrop.2010.04.005
21. Gericke, M.; Fardim, P.; Heinze, T. Ionic liquids--promising but challenging solvents for homogeneous derivatization of cellulose. *Molecules* **2012**, *17*, 7458– 7502, DOI: 10.3390/molecules17067458
22. Xie, H.; Yu, X.; Yang, Y.; Zhao, Z. K. Capturing CO_2 for cellulose dissolution. *Green Chem.* **2014**, *16*, 2422– 2427, DOI: 10.1039/C3GC42395F
23. Zhang, Q.; Oztekin, N. S.; Barrault, J.; De Oliveira Vigier, K.; Jérôme, F. Activation of microcrystalline cellulose in a CO_2-based switchable system. *ChemSusChem* **2013**, *6*, 593– 596, DOI: 10.1002/cssc.201200815
24. Yang, Y.; Xie, H.; Liu, E. Acylation of cellulose in reversible ionic liquids. *Green Chem.* **2014**, *16*, 3018– 3023, DOI: 10.1039/C4GC00199K
25. Song, L.; Yang, Y.; Xie, H.; Liu, E. Cellulose Dissolution and In Situ Grafting in a Reversible System using an Organocatalyst and Carbon Dioxide. *ChemSusChem* **2015**, *8*, 3217– 3221, DOI: 10.1002/cssc.201500378
26. Söyler, Z.; Onwukamike, K. N.; Grelier, S.; Grau, E.; Cramail, H.; Meier, M. A. R. Sustainable succinylation of cellulose in a CO_2 -based switchable solvent and subsequent Passerini 3-CR and Ugi 4-CR modification. *Green Chem.* **2018**, *20*, 214– 224, DOI: 10.1039/C7GC02577G
27. Llevot, A.; Dannecker, P.-K.; von Czapiewski, M.; Over, L. C.; Söyler, Z.; Meier, M. A. R. Renewability is not Enough: Recent Advances in the Sustainable Synthesis of Biomass-Derived Monomers and Polymers. *Chem. - Eur. J.* **2016**, *22*, 11510– 11521, DOI: 10.1002/chem.201602068
28. Schenzel, A.; Hufendiek, A.; Barner-Kowollik, C.; Meier, M. A. R. Catalytic transesterification of cellulose in ionic liquids: Sustainable access to cellulose esters. *Green Chem.* **2014**, *16*, 3266– 3271, DOI: 10.1039/c4gc00312h
29. Kulomaa, T.; Matikainen, J.; Karhunen, P.; Heikkilä, M.; Fiskari, J.; Kilpeläinen, I. Cellulose fatty acid esters as sustainable film materials – effect of side chain structure on barrier and mechanical properties. *RSC Adv.* **2015**, *5*, 80702– 80708, DOI: 10.1039/C5RA12671A
30. Wang, P.; Tao, B. Y. Synthesis of cellulose-fatty acid esters for use as biodegradable plastics. *J. Environ. Polym. Degr.* **1995**, *3*, 115– 119, DOI: 10.1007/BF02067487
31. Söyler, Z.; Meier, M. A. R. Catalytic Transesterification of Starch with Plant Oils: A Sustainable and Efficient Route to Fatty Acid Starch Esters. *ChemSusChem* **2017**, *10*, 182– 188, DOI: 10.1002/cssc.201601215
32. Dankovich, T. A.; Hsieh, Y.-L. Surface modification of cellulose with plant triglycerides for hydrophobicity. *Cellulose* **2007**, *14*, 469– 480, DOI: 10.1007/s10570-007-9132-1
33. King, A. W. T.; Jalomäki, J.; Granström, M.; Argyropoulos, D. S.; Heikkinen, S.; Kilpeläinen, I. A new method for rapid degree of substitution and purity determination of chloroform-soluble cellulose esters, using ^{31}P NMR. *Anal. Methods* **2010**, *2*, 1499– 1505, DOI: 10.1039/c0ay00336k
34. Villiers, C.; Dognon, J.-P.; Pollet, R.; Thuéry, P.; Ephritikhine, M. An isolated CO_2 adduct of a nitrogen base: Crystal and electronic structures. *Angew. Chem., Int. Ed.* **2010**, *49*, 3465– 3468, DOI: 10.1002/anie.201001035

35. Onwukamike, K. N.; Tassaing, T.; Grelier, S.; Grau, E.; Cramail, H.; Meier, M. A. R. Detailed Understanding of the DBU/CO_2 Switchable Solvent System for Cellulose Solubilization and Derivatization. *ACS Sustainable Chem. Eng.* **2018**, *6*, 1496– 1503, DOI: 10.1021/acssuschemeng.7b04053

Supporting Information for:

Sustainable Transesterification of Cellulose with high oleic sunflower oil in a DBU-CO_2 Switchable Solvent

Kelechukwu N. Onwukamike,[a,b] Stéphane Grelier,[b] Etienne Grau,[b] Henri Cramail,[b] Michael A.R. Meier[a*]*

[a] Institute of Organic Chemistry (IOC), Materialwissenschaftliches Zentrum (MZE), Karlsruhe Institute of Technology (KIT), Straße am Forum 7, 76131 Karlsruhe, Germany

[b] Laboratoire de Chimie des Polymères Organiques, Université de Bordeaux, UMR5629, CNRS - Bordeaux INP - ENSCBP, 16 Avenue Pey-Berland, 33607 Pessac Cedex France

Number of pages: 15; Number of Figures: 27; Number of Table: 1

SI. I FT-IR Optimization study of transesterification reaction on microcrystalline cellulose (MCC) using high oleic sunflower oil.

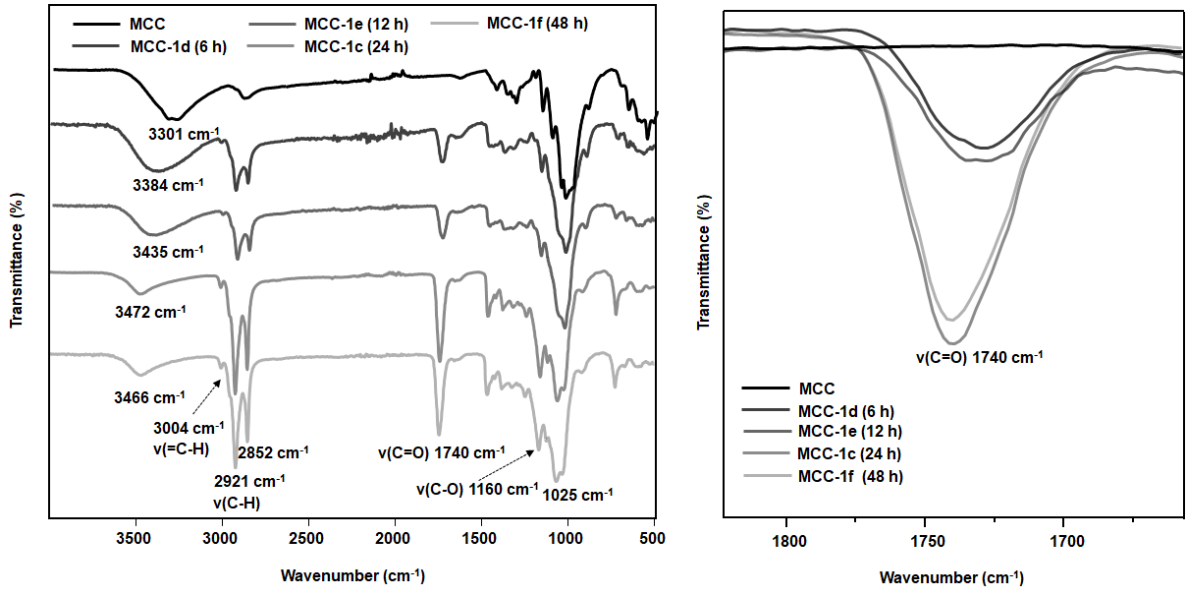

Figure S1: FT-IR spectra of FACEs at various reaction time: MCC-1d (6 h), MCC-1e (12 h), MCC-1c (24 h), MCC-1f (48 h). (5 wt. (%) cellulose (MCC), 3 eq. high oleic sunflower oil/AGU cellulose, 115 °C).

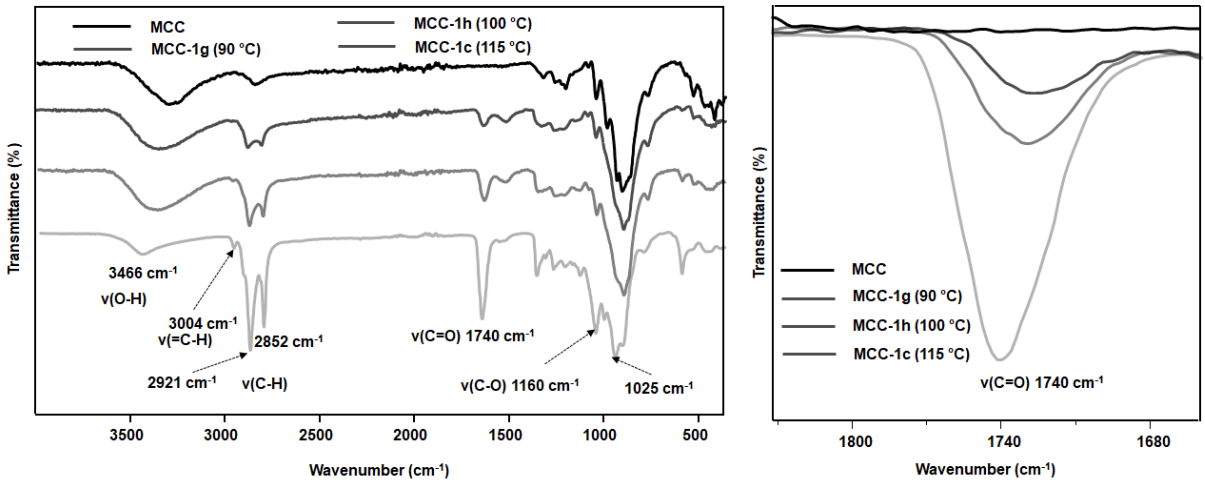

Figure S2: FT-IR spectra of FACEs at various reaction temperature: MCC-1g (90 °C), MCC-1h (100 °C), MCC-1c (115 °C). (5 wt. (%) cellulose (MCC), 3eq. high oleic sunflower oil/AGU cellulose, 24 h).

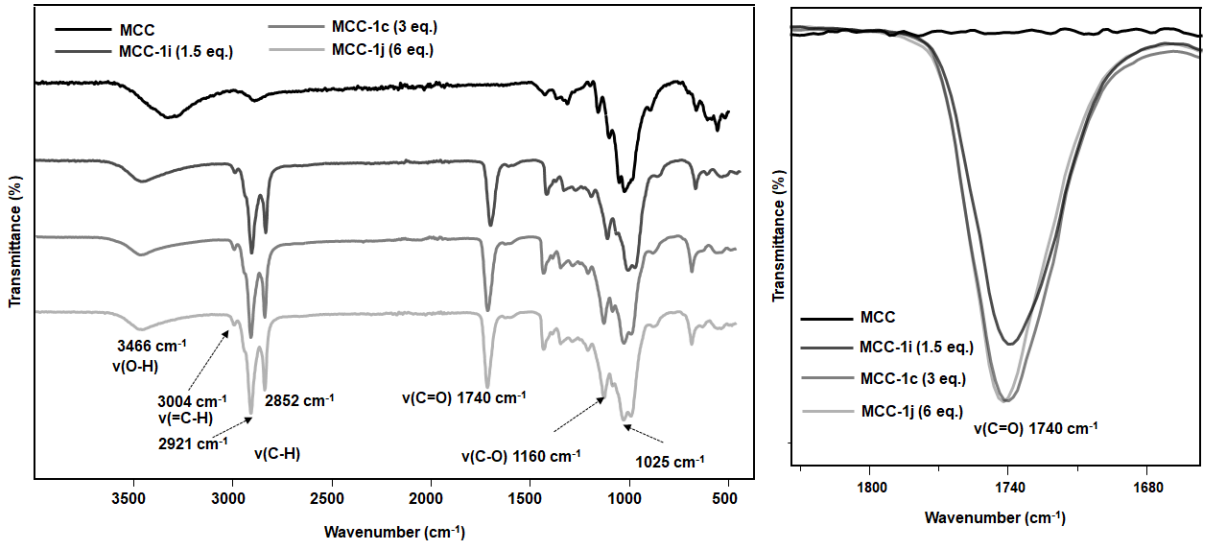

Figure S3: FT-IR spectra of FACEs at various plant high oleic sunflower oil equivalents: MCC-1i (1.5 eq./AGU), MCC-1c (3 eq./AGU), MCC-1j (6 eq./AGU). (5 wt. (%) cellulose 115 °C, 24 h).

SI II: ^{31}P NMR for DS determination of FACEs from microcrystalline cellulose (MCC)

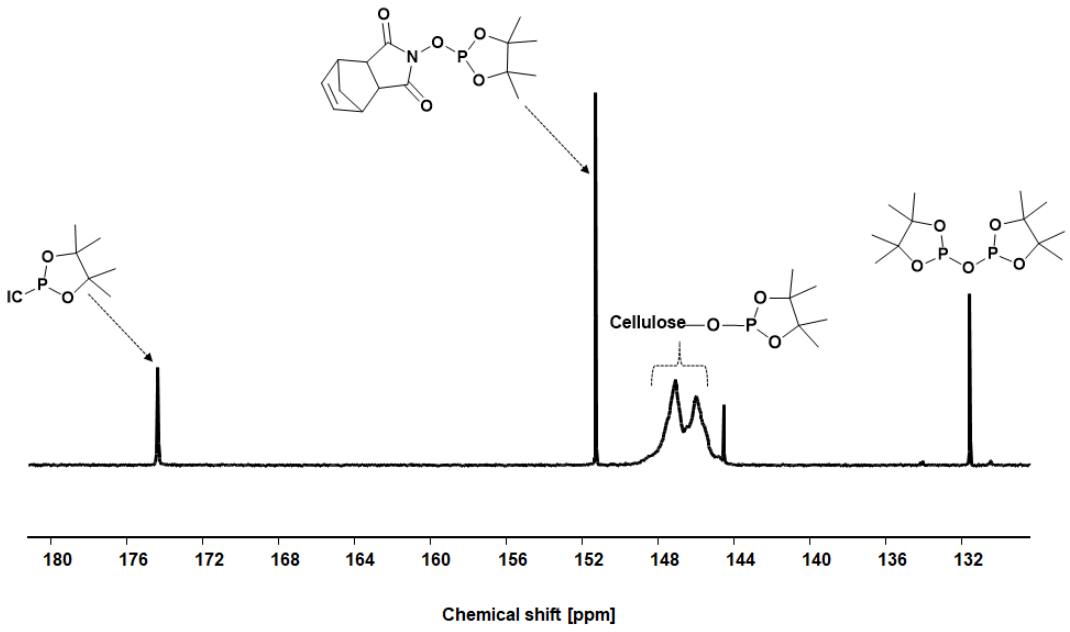

Figure S4: ^{31}P NMR ($CDCl_3$), 400 MHz, 1024 scans: Determination of degree of substitution (DS) of FACE (MCC-1d). (5 wt. (%) MCC, 3 eq. high oleic sunflower oil/AGU, 115 °C, 6 h).

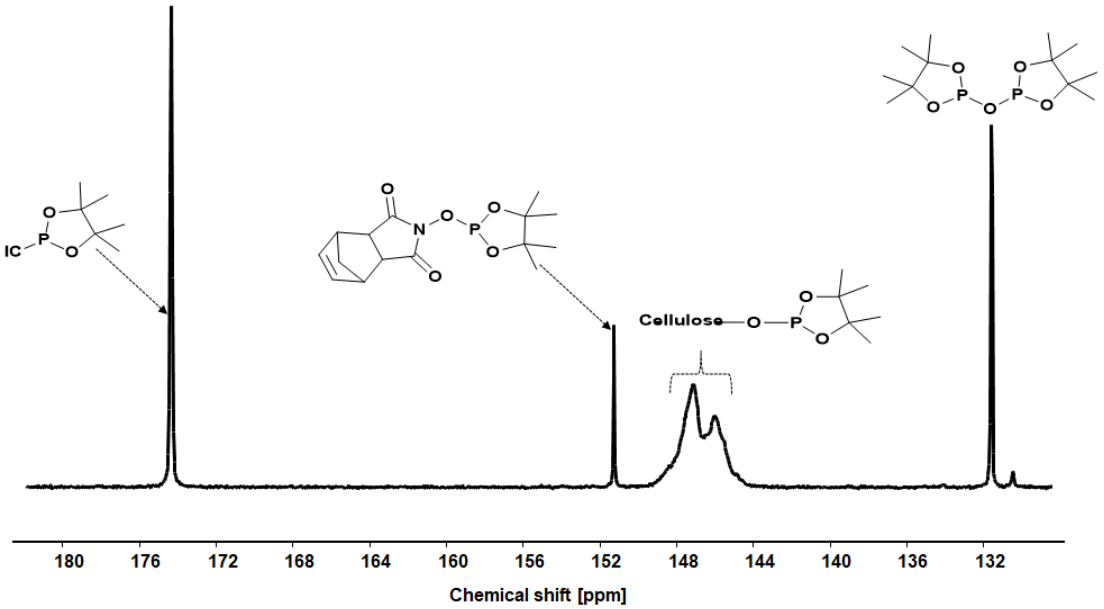

Figure S5: ^{31}P NMR ($CDCl_3$), 400 MHz, 1024 scans: Determination of degree of substitution (DS) of FACE (MCC-1e). (5 wt. (%) MCC, 3 eq. high oleic sunflower oil/AGU, 115 °C, 12 h).

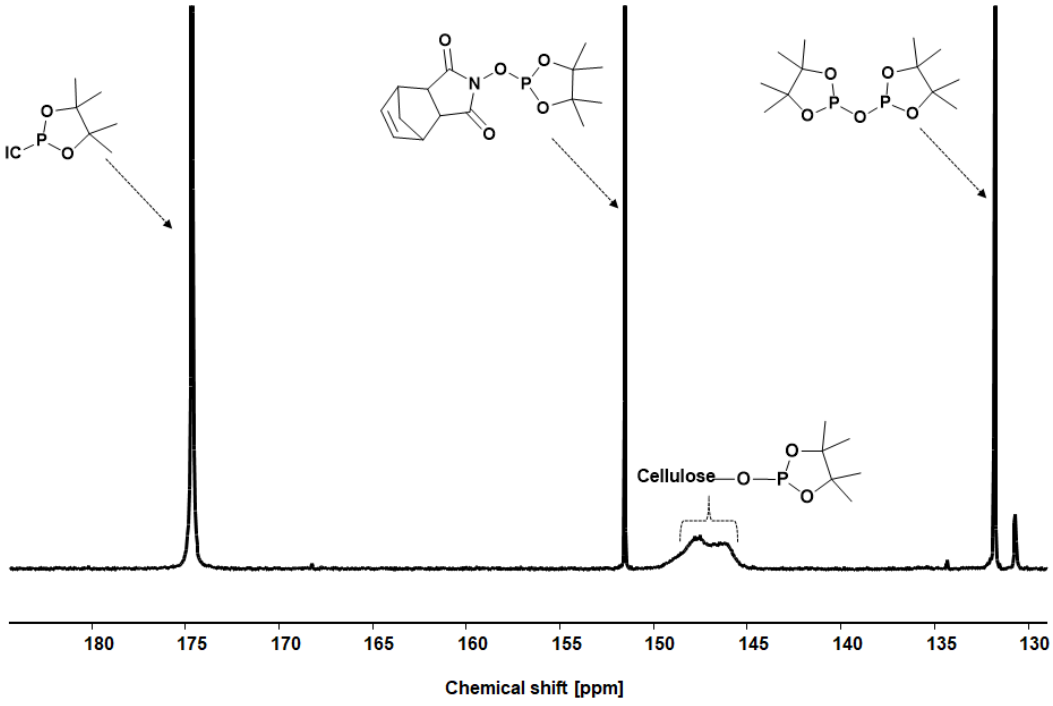

Figure S6: ^{31}P NMR ($CDCl_3$), 400 MHz, 1024 scans: Determination of degree of substitution (DS) of FACE (MCC-1c). (5 wt. (%) MCC, 3 eq. high oleic sunflower oil/AGU, 115 °C, 24 h).

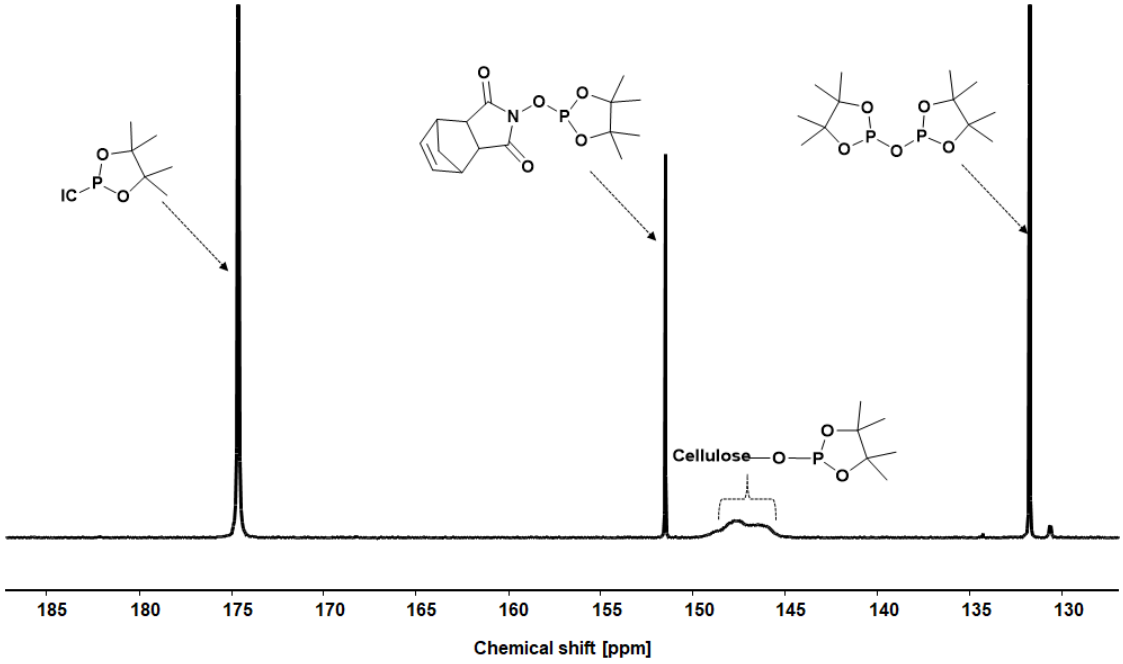

Figure S7: ^{31}P NMR ($CDCl_3$), 400 MHz, 1024 scans: Determination of degree of substitution (DS) of FACE (MCC-1c). (5 wt. (%) MCC, 3 eq. high oleic sunflower oil/AGU, 115 °C, 48 h).

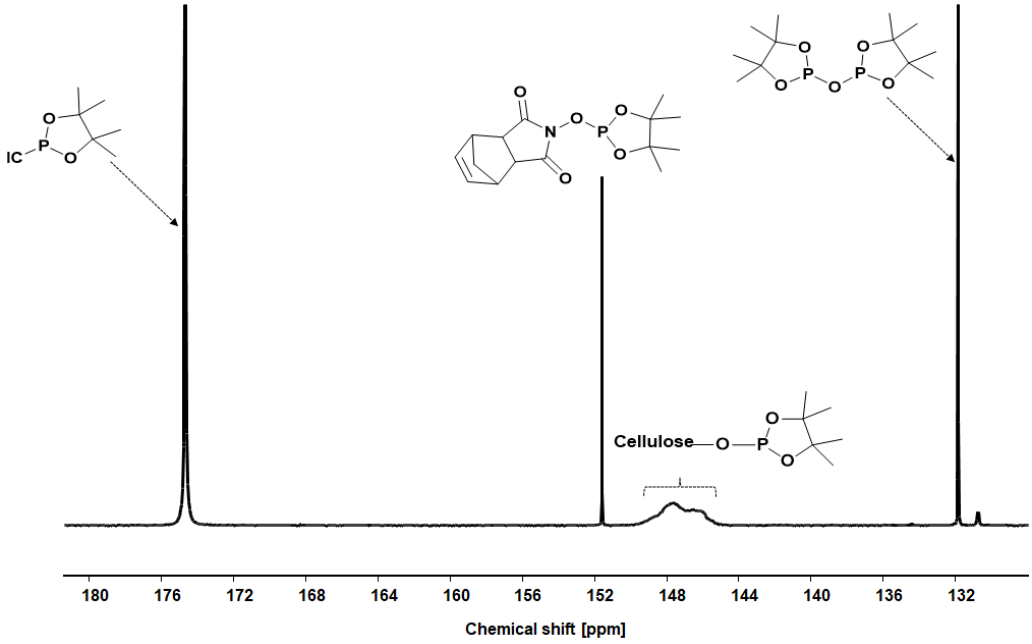

Figure S8: ^{31}P NMR ($CDCl_3$), 400 MHz, 1024 scans: Determination of degree of substitution (DS) of FACE (MCC-1i). (5 wt. (%) MCC, 1.5 eq. high oleic sunflower oil/AGU, 115 °C, 24 h)

Table S1: Control of degree of substitution (DS) of FACE with reaction time.

Sample	Reaction time	DS
MCC-1d	6 h	0.34
MCC-1e	12 h	0.50
MCC-1c	24 h	1.59
MCC-1f	48 h	1.44

Reaction conditions: 3 eq. high oleic sunflower oil per AGU cellulose (MCC), 5 wt. % MCC, 115 °C (DS calculated from ^{31}P NMR).

SI III: FT-IR spectra of FACEs from cellulose filter paper (FP) and cellulose pulp (CP)

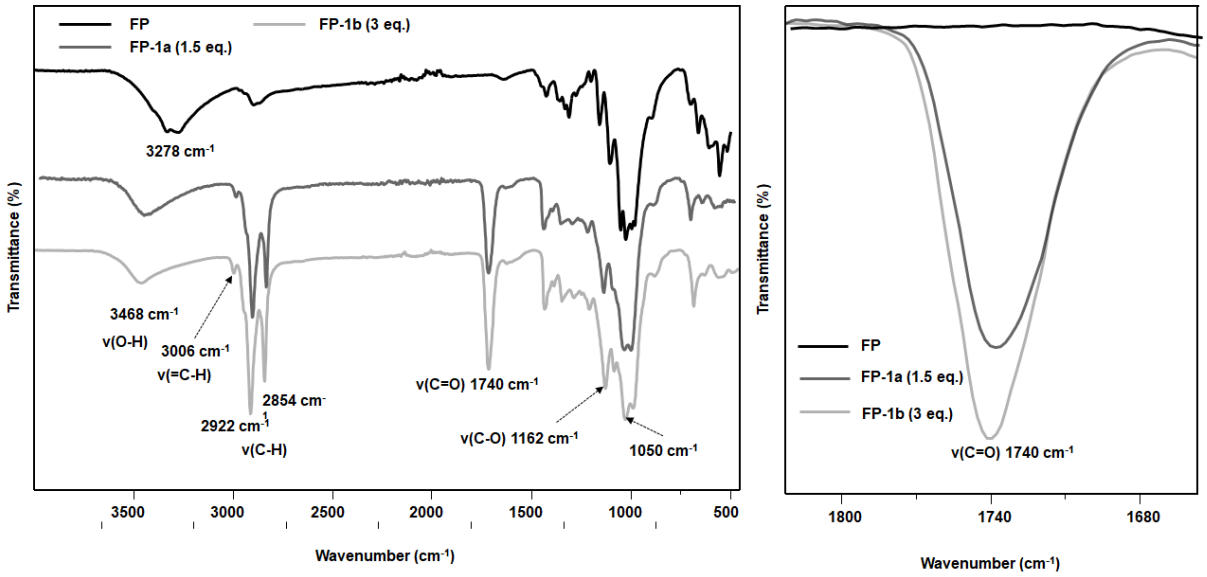

Figure S9: FT-IR spectra of FACEs at various plant high oleic sunflower oil equivalents: FP-1a (1.5 eq./AGU), FP-1b (3 eq./AGU, 5 wt. (%) cellulose Whatman™ filter paper No. 5, 115 °C, 24 h).

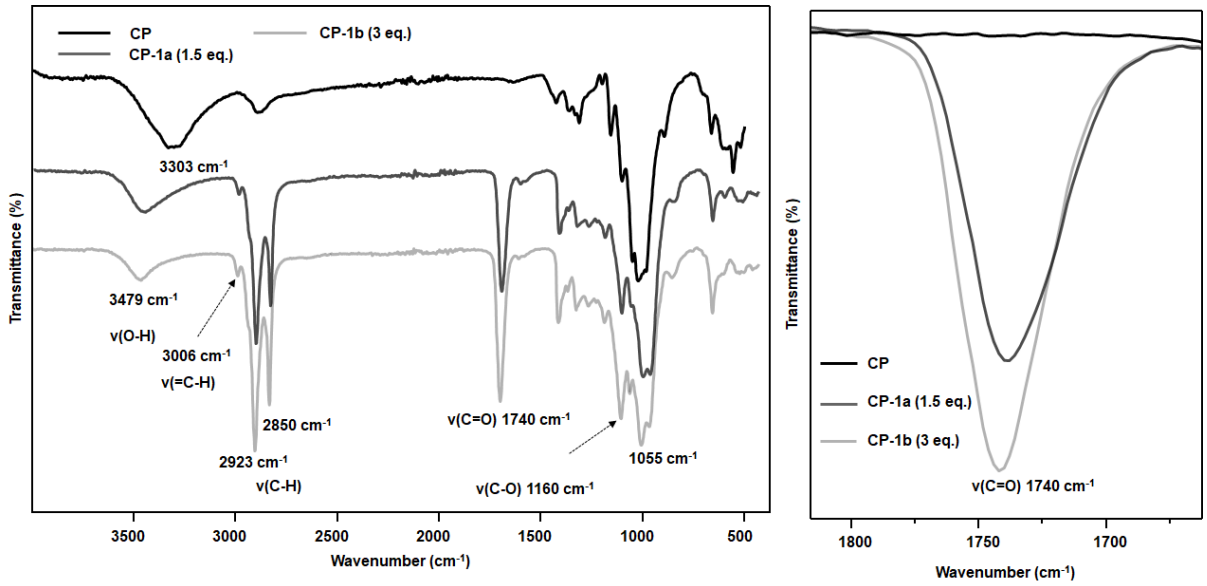

Figure S10: FT-IR spectra of FACEs at various plant high oleic sunflower oil equivalents: CP-1a (1.5 eq./AGU), CP-1b (3 eq./AGU, 5 wt. (%) cellulose pulp, 115 °C, 24 h)

SI IV: ^{1}H and ^{13}C NMR of FACEs

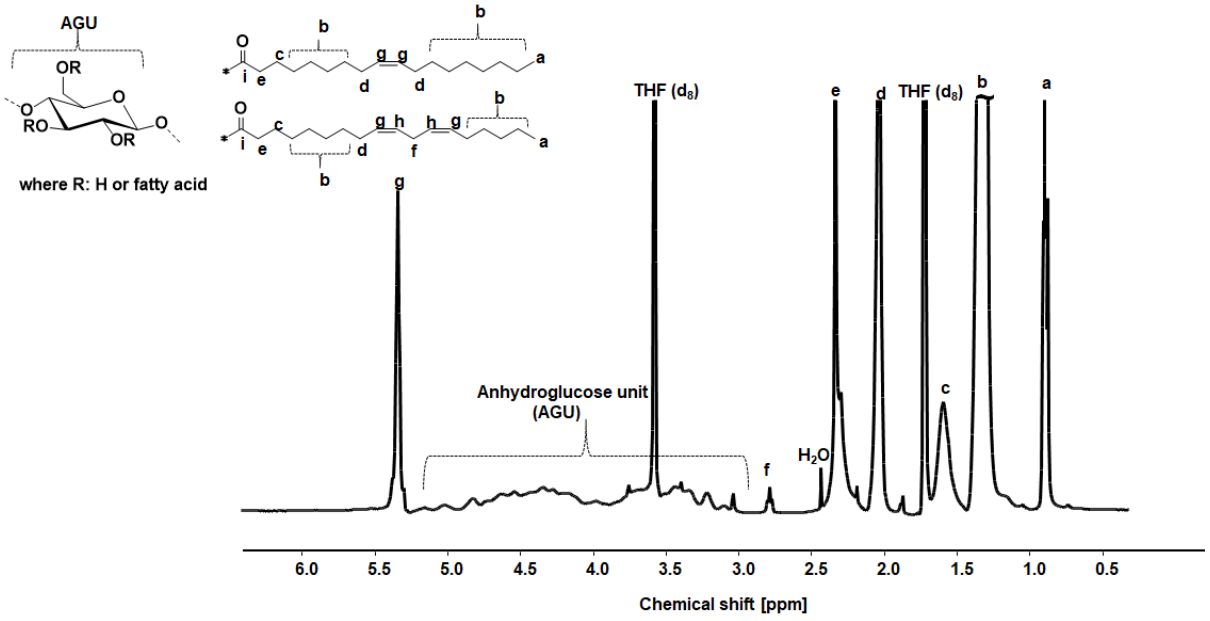

Figure S11a: ^{1}H NMR (THF, d_8), 400 MHz, 1024 scans at 50 °C for FACE: MCC-1c. (5 wt. (%) MCC, 3 eq. high oleic sunflower oil/AGU, 115 °C, 24 h).

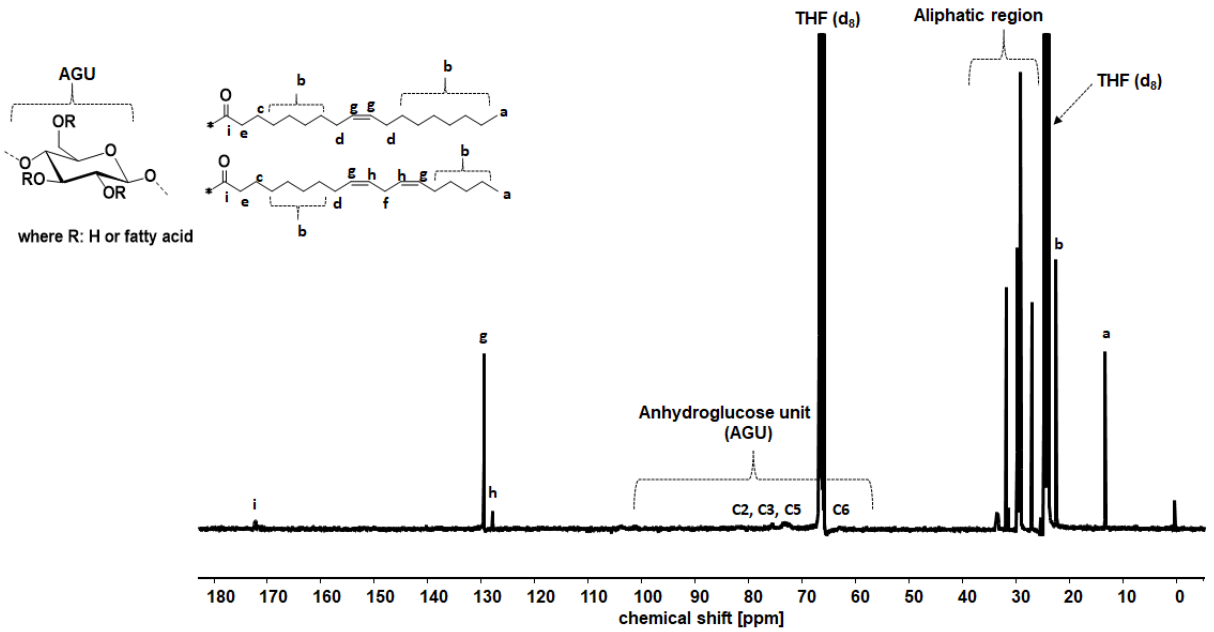

Figure S11b: ^{13}C NMR (THF, d_8), 100 MHz, 6000 scans at 50 °C for FACE: MCC-1c. (5 wt. (%) MCC, 3 eq. high oleic sunflower oil/AGU, 115 °C, 24 h).

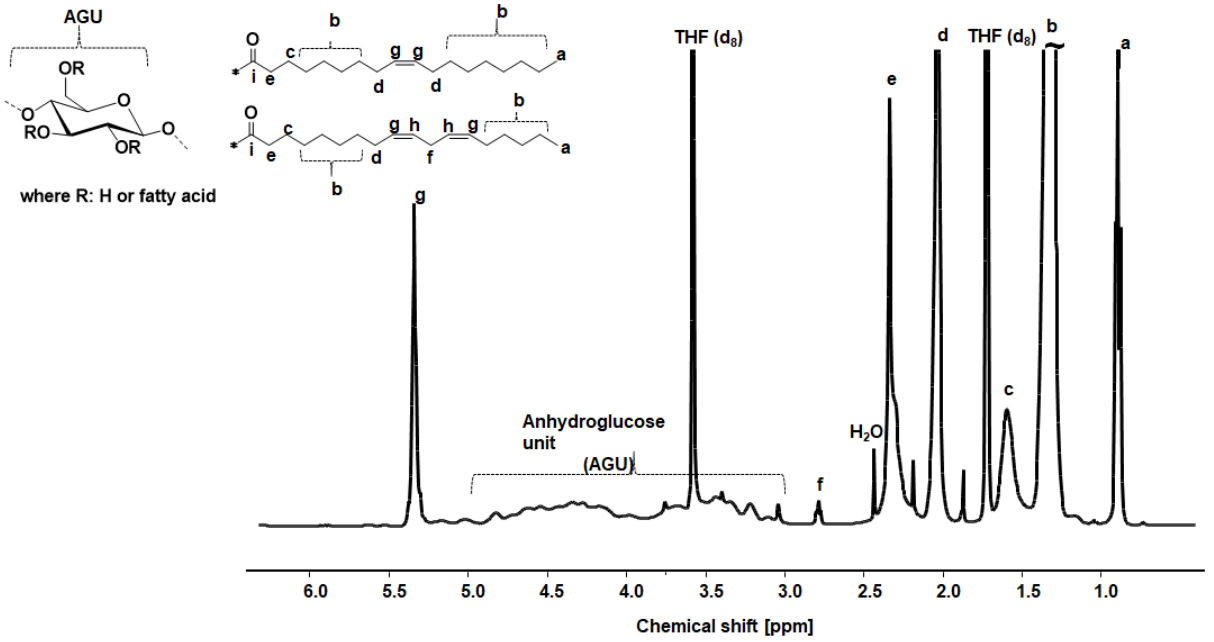

Figure S12a: ^{1}H NMR (THF, d_8), 400 MHz, 1024 scans at 50 °C for FACE: FP-1b. (5 wt. (%) cellulose Whatman™ filter paper No. 5 (FP), 3 eq. high oleic sunflower oil/AGU, 115 °C, 24 h).

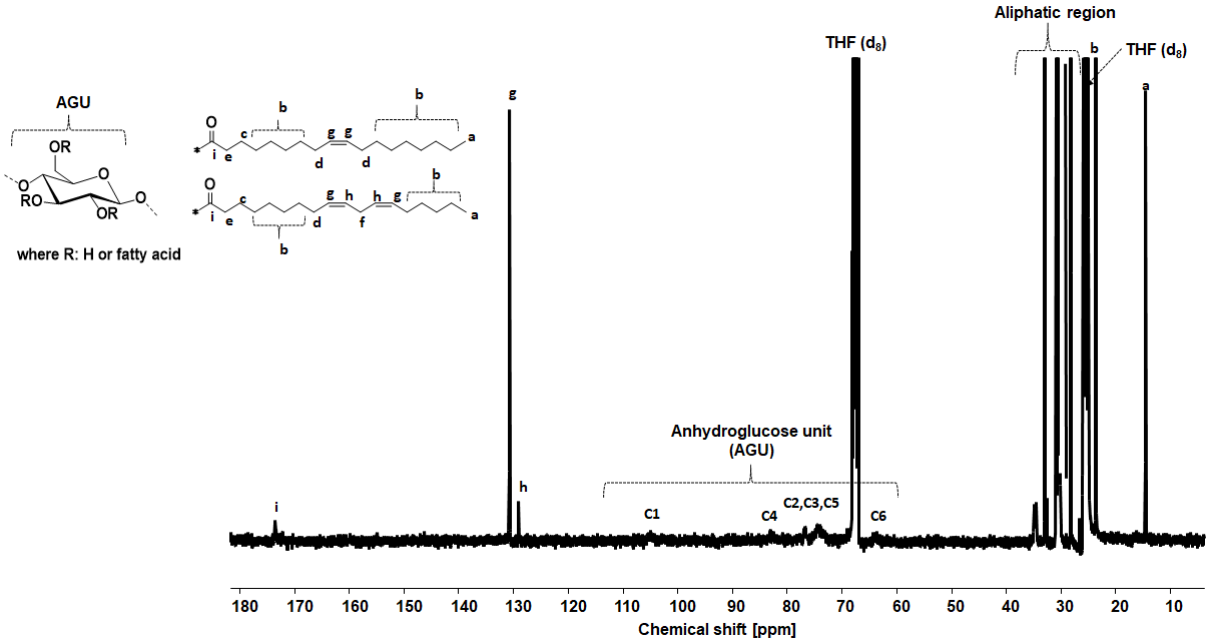

Figure S12b: ^{13}C NMR (THF, d_8), 100 MHz, 6000 scans at 50 °C for FACE: FP-1b. (5 wt. (%) cellulose Whatman™ filter paper No. 5 (FP), 3 eq. high oleic sunflower oil/AGU, 115 °C, 24 h).

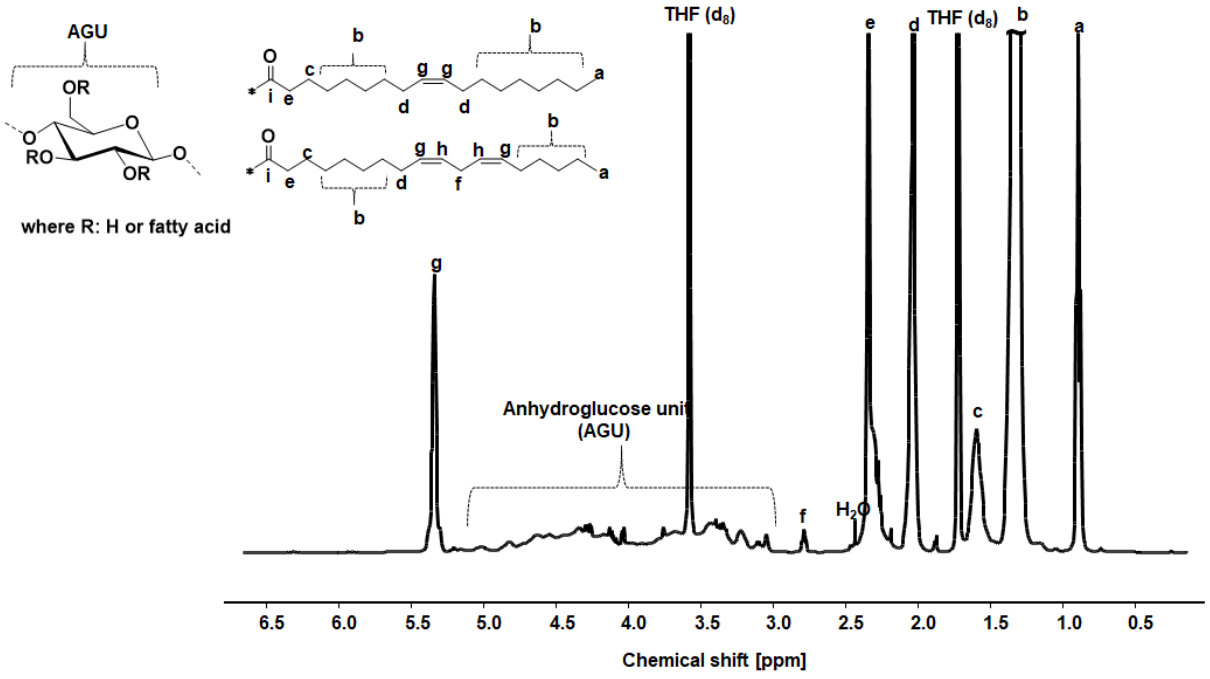

Figure S13a: ^{1}H NMR (THF, d_8), 400 MHz, 1024 scans at 50 °C for FACE: CP-1b. (5 wt. (%) cellulose pulp (CP), 3 eq. high oleic sunflower oil/AGU, 115 °C, 24 h).

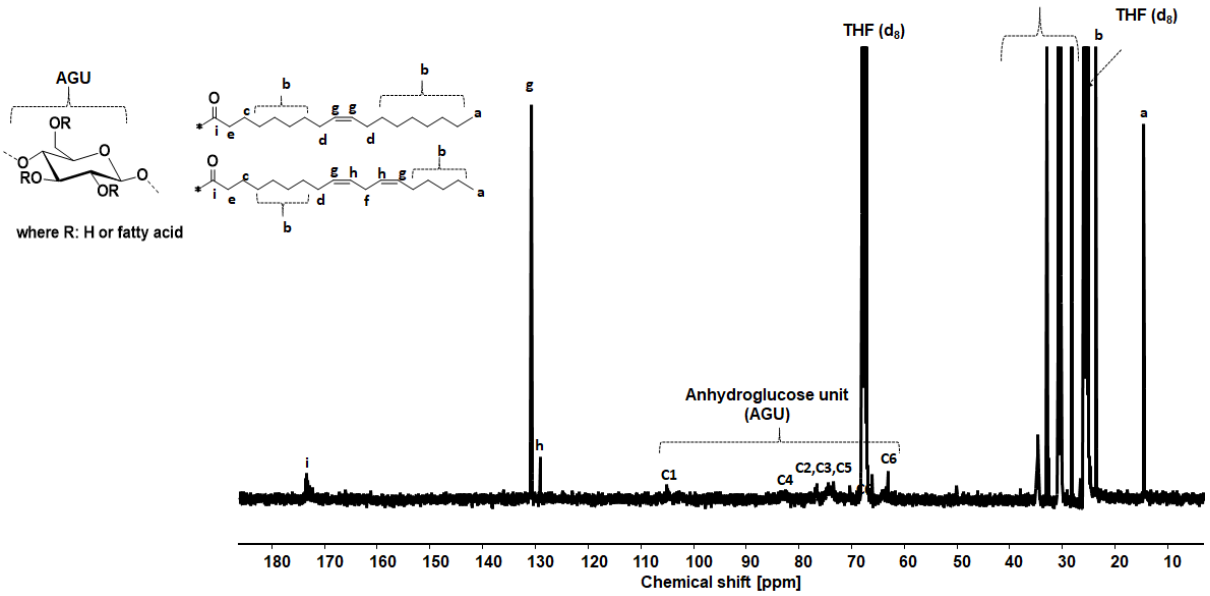

Figure S13b: ^{1}H NMR (THF, d_8), 100 MHz, 6000 scans at 50 °C for FACEs. (5 wt. (%) cellulose pulp (CP), 3 eq. high oleic sunflower oil/AGU, 115 °C, 24 h).

SI V: ^{31}P NMR for DS determination of FACEs of cellulose filter paper (FP) and cellulose pulp (CP)

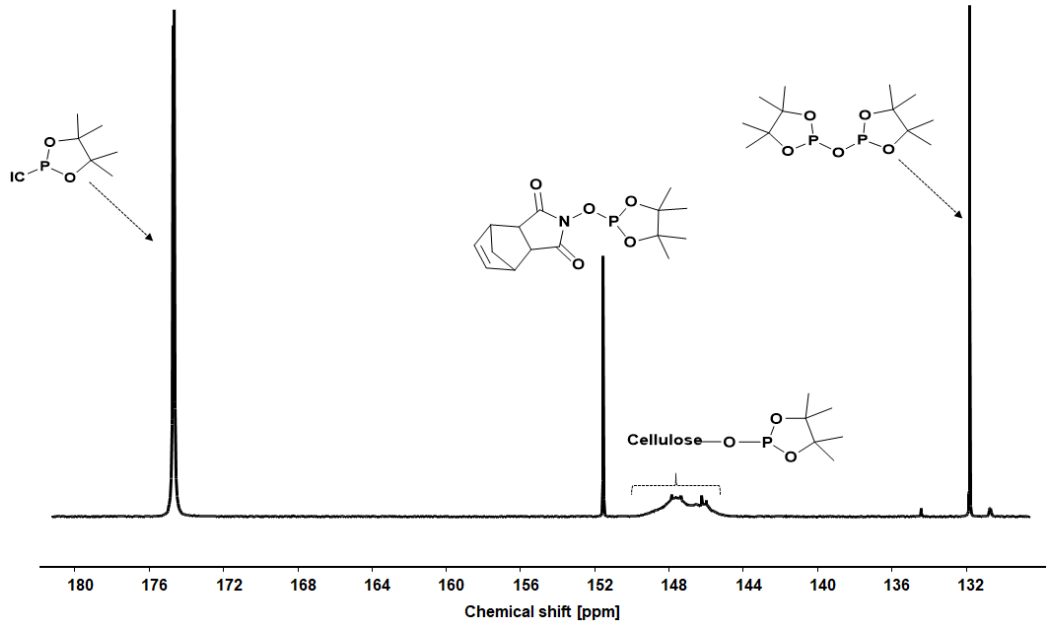

Figure S14: ^{31}P NMR ($CDCl_3$), 400 MHz, 1024 scans determination of degree of substitution (DS) of fatty acid cellulose esters (FACE): FP-1a. (5 wt. (%) cellulose Whatman™ filter paper No. 5 (FP) 1.5 eq. high oleic sunflower oil/AGU, 115 °C, 24 h).

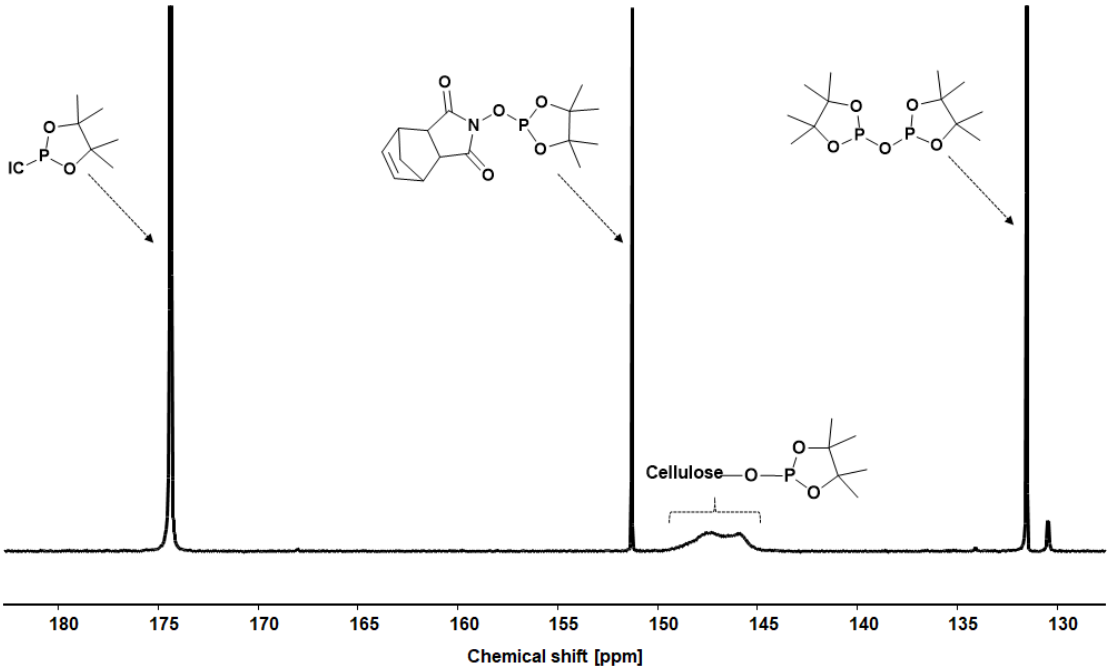

Figure S15: ^{31}P NMR ($CDCl_3$), 400 MHz, 1024 scans determination of degree of substitution (DS) of FACE: FP-1b. (5 wt. (%) cellulose Whatman™ filter paper No. 5 (FP) 3 eq. high oleic sunflower oil/AGU, 115 °C, 24 h).

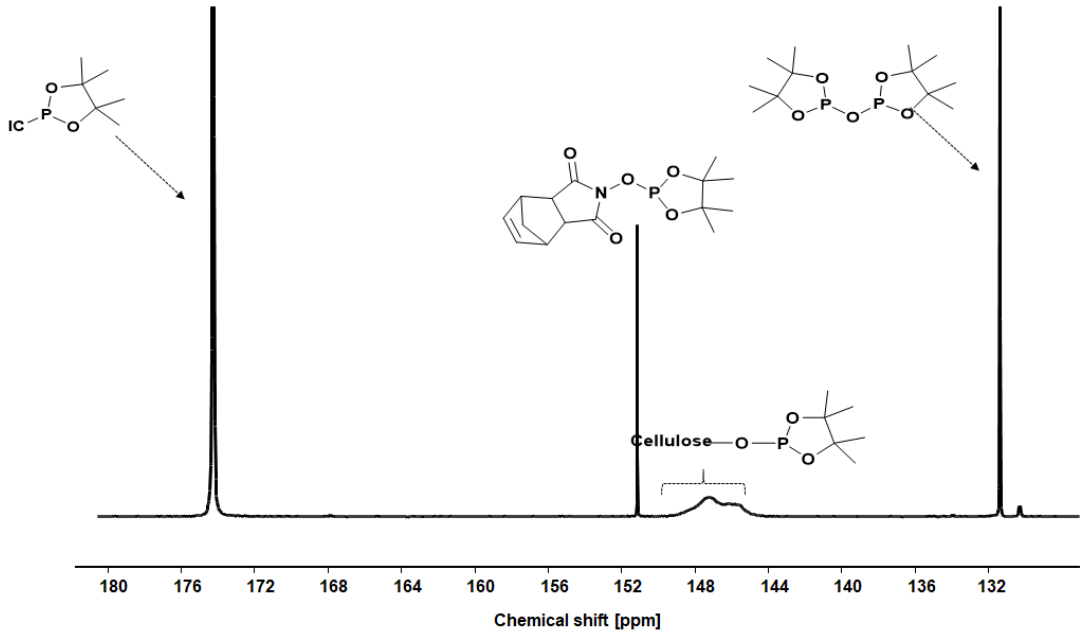

Figure S16: ^{31}P NMR ($CDCl_3$), 400 MHz, 1024 scans determination of degree of substitution (DS) of FACE: CP-1a. (5 wt. (%) cellulose pulp, (CP) 1.5 eq. high oleic sunflower oil/AGU, 115 °C, 24 h).

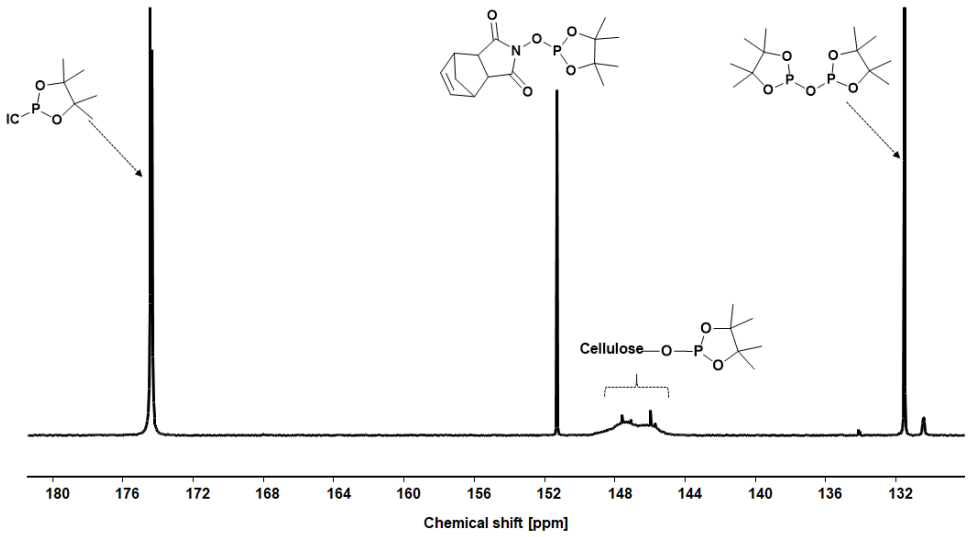

Figure S17: ^{31}P NMR ($CDCl_3$), 400 MHz, 1024 scans determination of degree of substitution (DS) of FACE: CP-1b. (5 wt. (%) cellulose pulp, (CP) 3 eq. high oleic sunflower oil/AGU, 115 °C, 24 h).

SI VI: SEC traces (DMAc-LiBr) of lower DS (around 1.0) FACEs

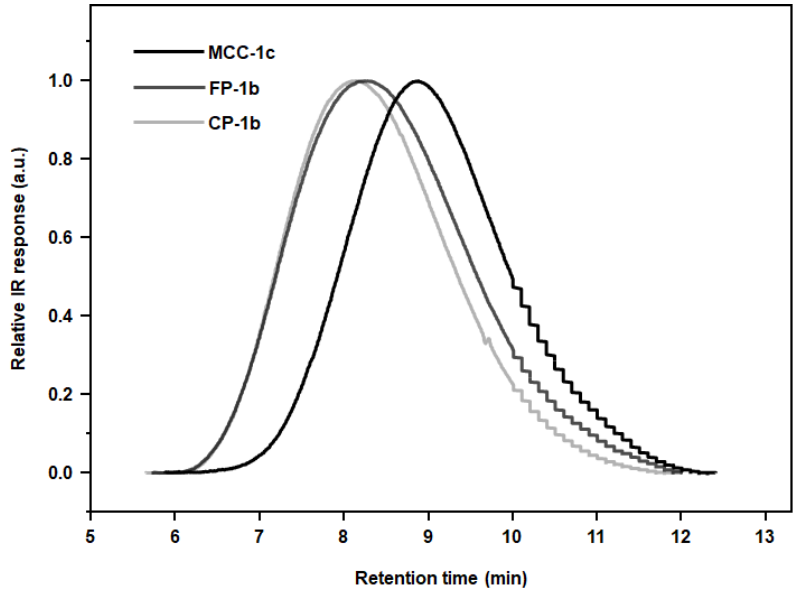

Figure S18: SEC traces (DMAc-LiBr) comparison of FACEs from microcrystalline cellulose (MCC-1i; DS 1.06), Whatman™ filter paper No. 5 (FP-1a; DS 1.02) and cellulose pulp (CP-1a; DS 1.08).

SI VII: XRD patterns of FACEs of cellulose filter paper (FP) and cellulose pulp (CP)

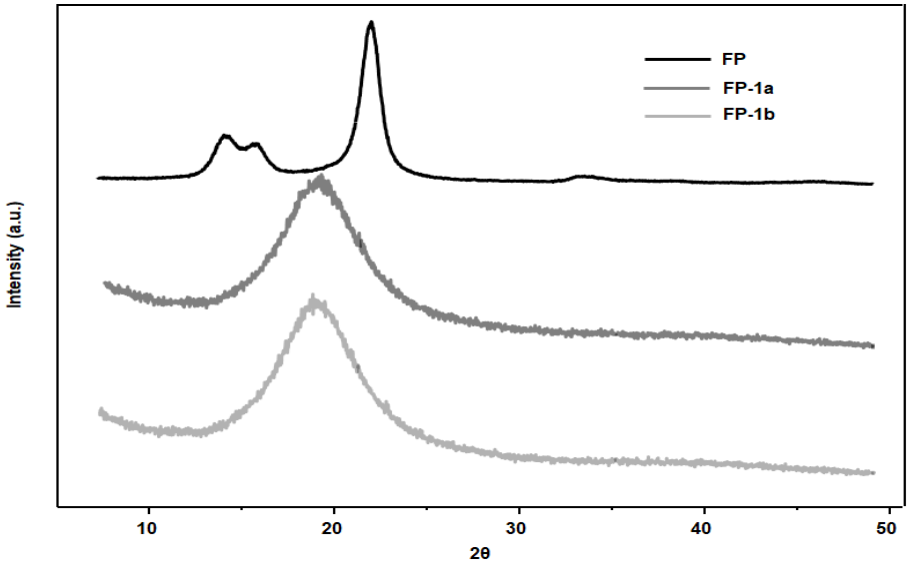

Figure S19: X-ray diffraction pattern of cellulose Whatman™ filter paper No. 5 (FP) and resulting FACEs from FP (FP-1a, FP-1b) (5 wt. (%) cellulose, 24 h,115 °C).

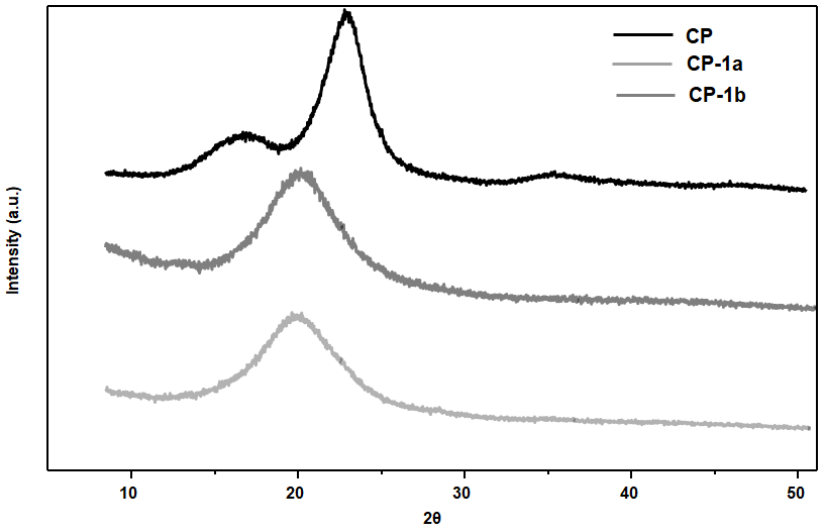

Figure S20: X-ray diffraction pattern of cellulose pulp (CP) and resulting FACEs from cellulose pulp (CP-1a, CP-1b) (5 wt. (%) cellulose, 24 h, 115 °C).

SI VIII: TGA analysis of FACEs of microcrystalline cellulose (MCC), filter paper (FP) and cellulose pulp (CP)

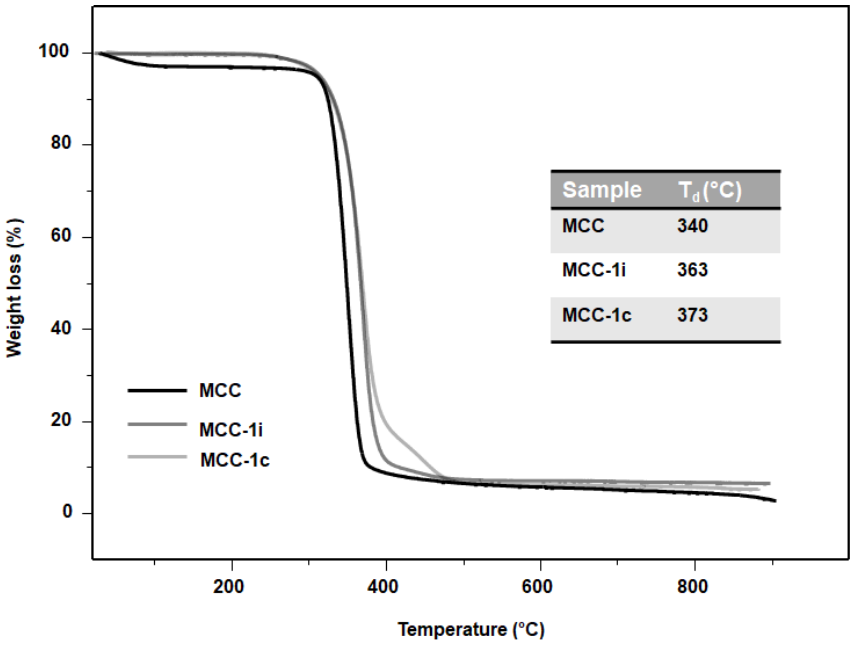

Figure S21: Thermogravimetric analysis (TGA) of microcrystalline cellulose (MCC) and resulting FACEs from MCC (MCC-1c, MCC-1i) (5 wt. (%) cellulose, 24 h, 115 °C).

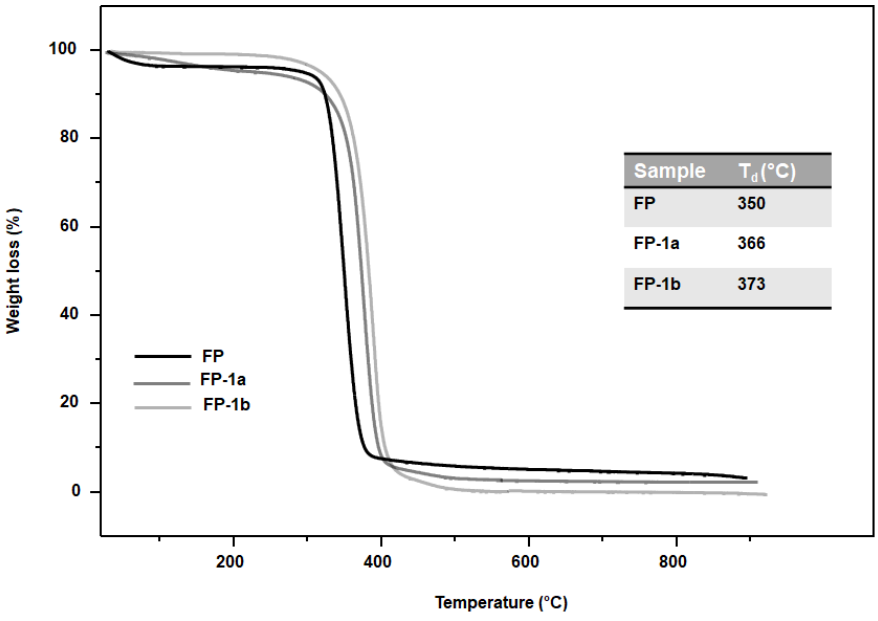

Figure S22: Thermogravimetric analysis (TGA) of cellulose Whatman™ filter paper No. 5 (FP) and resulting FACEs from FP (FP-1a, FP-1b) (5 wt. (%) cellulose, 24 h, 115 °C).

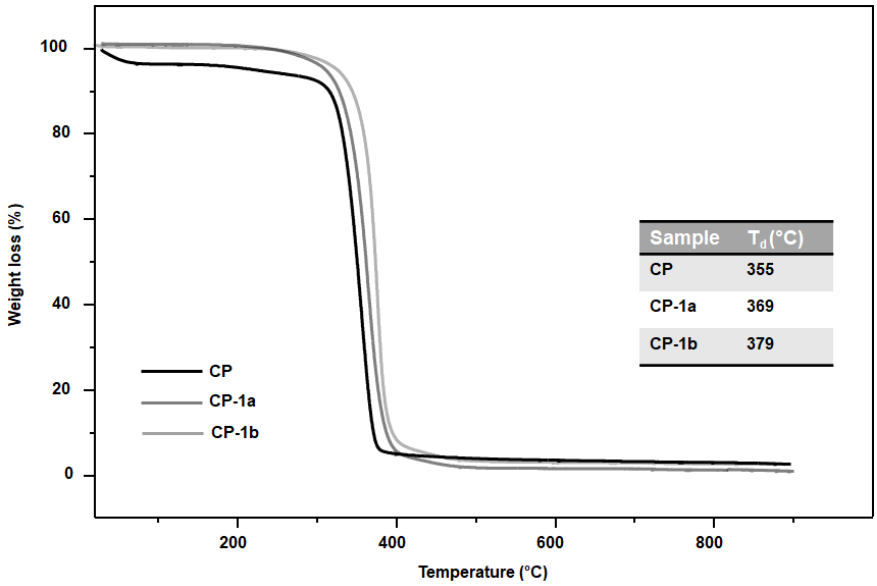

Figure S23: Thermogravimetric analysis (TGA) of cellulose pulp (CP) and resulting FACEs from CP (CP-1a, CP-1b) (5 wt. (%) cellulose, 24 h, 115 °C).

SI IX: TGA analysis of FACEs films

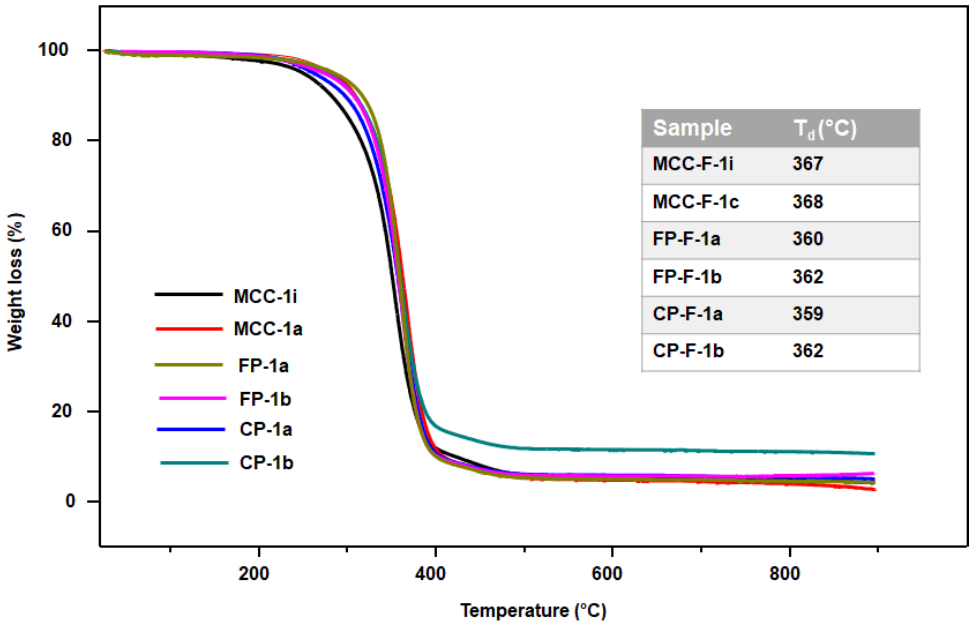

Figure S24: Thermogravimetric analysis (TGA) of FACEs films (MCC-F-1i, MCC-F-1c, FP-F-1a, FP-F-1b, CP-F-1a, CP-F-1b).